

Copyright © 1976, by the author(s).
All rights reserved.

Permission to make digital or hard copies of all or part of this work for personal or classroom use is granted without fee provided that copies are not made or distributed for profit or commercial advantage and that copies bear this notice and the full citation on the first page. To copy otherwise, to republish, to post on servers or to redistribute to lists, requires prior specific permission.

ON THE SPATIAL BREADTH OF SPATIAL FREQUENCY
CHANNELS IN HUMAN VISUAL DETECTION

by

Matthew C. Halter

Memorandum No. ERL-M609

4 November 1976

ELECTRONICS RESEARCH LABORATORY

College of Engineering
University of California, Berkeley
94720

ON THE SPATIAL BREADTH OF SPATIAL FREQUENCY
CHANNELS IN HUMAN VISUAL DETECTION

Matthew C. Halter

ABSTRACT

In recent years several investigators have shown that the process of human visual detection can be modelled with a series of independent, parallel detection mechanisms called channels. Early evidence showed that these channels are frequency selective. This means that each is sensitive only to spatial intensity patterns which contain sinusoidal grating components in the channel's frequency band. More recent evidence indicates that channels are also spatially selective. That is that the detection of a sinusoidal grating is accomplished by the combined action of several channels each of which is selectively sensitive to a single striation of the grating.

The present paper discusses a psychophysical experiment designed to test simultaneously both the frequency selectivity and spatial extent of these channels. Experimental stimuli contained either one or two half-field sinusoidal grating patches. Two spatial frequencies, 12.8 \sim /0 (cycles per degree) and 4.3 \sim /0, were used. In some two-patch stimuli the patches were at different frequencies. In others they were at the same frequency. Because responses to single patch stimuli were also measured, it was possible to calculate precisely the behavior which should have occurred whenever the two patches of a two-patch stimulus were detected independently. Thus, when the data for a two-patch stimulus did not agree with the appropriate independence calculation it was possible

to conclude that some single channel was sensitive to both patches.

Our findings support existing evidence that sinusoids at different frequencies are detected independently. Similarly, we find that two adjacent patches at 4.3 \sim /0 appear to be detected independently. This agrees with existing evidence that individual striations of such gratings are detected independently. Finally, we find that adjacent patches at 12.8 \sim /0 are detected far more easily than can be explained by the independent detection of each patch. This is taken to mean that the individual striations of sinusoidal gratings at this frequency are not detected independently. Instead, we conclude that there exists some single mechanism which is not only selective for this frequency but also sensitive to several cycles of the grating.



Committee Chairman

ACKNOWLEDGEMENTS

I wish to thank Professor David Sakrison for his help in all phases of this research. I also thank Cris Johnson and especially Daniel Swanson for their efforts as subjects and Barbara Kerekes and Doris Simpson for their help in preparing the final copy of this paper.

Research sponsored by the National Science Foundation Grants
ENG72-04198-A01/ENG75-10063.

TABLE OF CONTENTS

	PAGE NOS.
CHAPTER 1. INTRODUCTION	1
1.1. Research Objectives	1
1.2. Overview of the Dissertation	8
CHAPTER 2. THE FREQUENCY CHANNEL MODEL	10
2.1. A Description of the FCM	10
2.2. Evidence Supporting the FCM	15
2.3. The FCM as a Mathematical Model	20
2.4. Other Models and the Present Test of the FCM	22
CHAPTER 3. METHODS	29
3.1. Technique	29
3.2. The Probability Summation Calculation	34
3.3. Equipment	37
CHAPTER 4. STIMULI AND RESULTS	41
4.1. Stimuli	41
4.2. Data	46
4.3. Support for the Present Use of Average Ratings	53
CHAPTER 5. CONCLUSIONS	57
5.1. PSUM Comparisons - the Test for Independence	57
5.2. Criterion for Judgements on Goodness of Fit	59
5.3. Conclusions Regarding the Modelling of Visual Detection	61
APPENDIX. OTHER EXPERIMENTS	66
A.1. Patches	68
A.2. Patches II	71
A.3. Channel Shift-Phase I	74
A.4. Channel Shift-Phase II	77
A.5. "p"	77
A.6. Coherence	80
A.7. Spacing	87
A.8. Anticipation	87
REFERENCES	94

CHAPTER 1

INTRODUCTION

1.1. Research Objectives

MOTIVATION: The basic consideration in this research is the engineering problem of modelling human perception of distortion in visual stimuli for the purpose of image communication system design.

An image communication system is a device used to transmit visible information across space or time. Examples are television, video taping, photography, space photography and facsimile. In designing such a system the most straightforward objective would be physical perfection. Outputs should be physically identical to inputs. However, this objective is impossible with current technology. Physical systems always introduce distortion. Analog systems suffer from noise in their components (e.g. transistors and transmission media). Digital systems may transmit information error-free, but they require quantization of the input which is itself a distortion. Therefore, instead of physical perfection image transmission systems accomplish what might be called perceptual approximation. An output is considered satisfactory if its users perceive it to be sufficiently similar to the corresponding input.

The sufficiency of the perceptual approximation objective makes image transmission systems possible but has heretofore seen little use in optimizing them. Clearly, if an output need only look like the corresponding input, then an optimal system will transmit only those features of an input which are perceived by the user. Further, it will minimize distortion in those features only to the extent that the user requires. Television is an example of partial application of this principle. Signal bandwidth

and the spacing of adjacent lines have been chosen to match visual resolution. The time between frames has been chosen to match visual system response time. However, the considerations of this sort used in TV design form a very incomplete description of perception. The rest of the system was designed for physical perfection. For example, the light intensity at each point of the output is designed to mimic that at the input and the mean-square error of that approximation is used as the measure of system distortion.

Why is it that optimization according to perceptual considerations has not occurred? One can give the double answer that not enough is known about visual perception and that what is known is not known in the form of a mathematical model. Consider the phenomenon of lateral interaction. The sensed brightness at each point of the visual field is a function not only of light intensity at that point but also of the intensities at adjacent points. For example, if an image contains two light levels, dim on the left half and bright on the right with a rapid transition (dashed line in Fig. 1.1), then the perceived brightness distribution will have the form of the solid line of Fig. 1.1. The visual system amplifies such boundaries. This is the well-known Mach band effect (Ratliff [1]). Such an edge also has a "masking" effect. It causes a decrease in sensitivity to small intensity changes which occur near it (Fiorentini [2]). Thus, in transmitting such an image it would be more important to minimize the distortion away from the boundary than that near it. Unfortunately, most images contain many spatial patterns other than large, rapid intensity gradients like that of Fig. 1.1. If an image communication system is to optimally transmit arbitrary images, then its designer must know the lateral interactions resulting from arbitrary

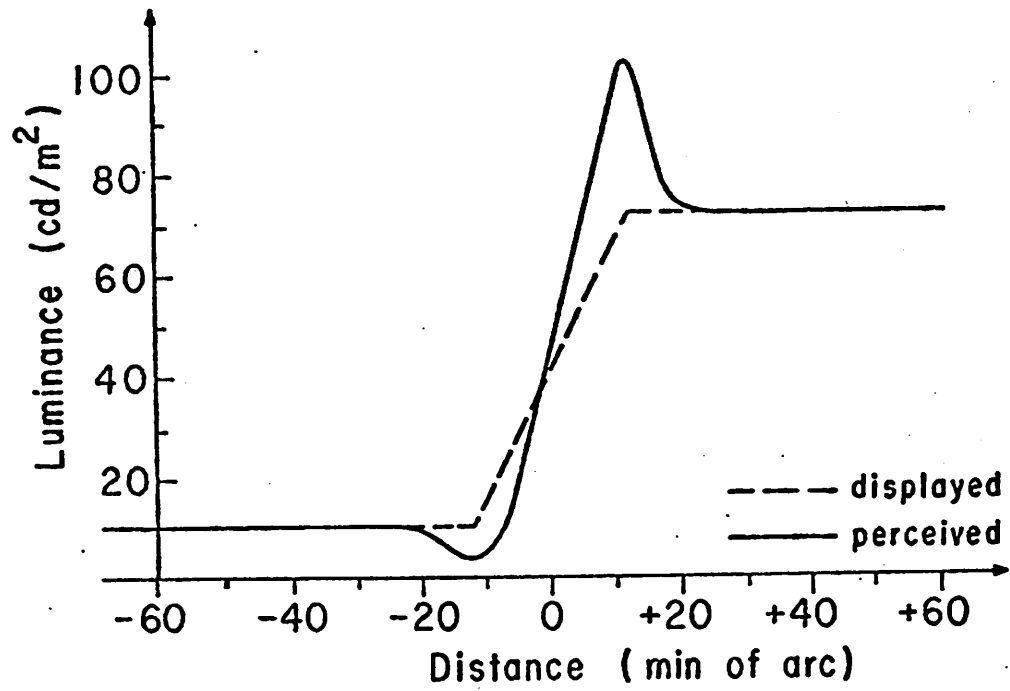


Fig. 1.1. The Mach band phenomenon.

intensity patterns. What is more, this knowledge must be useable as part of the system design process and, hence, must be in the form of a mathematical model. Such models are the designer's most essential tool. Properties of components are specified numerically (e.g. gain of a transistor, capacity of a communication channel). System structure (e.g. FM) and performance measures (e.g. rate-distortion theory) are known from and used via mathematical models.

This research concludes that a mathematical model for human visual perception is needed.

GOAL REDUCTION: Visual perception is a powerful and complex phenomenon. Scientific knowledge and technique have not yet progressed to a point where extensive modelling seems possible. Hence, this study is restricted to a test of the Frequency Channel Model of detection.

A normal adult gathers more information with his vision than with any of his other senses. With it he can recognize countless objects and discern much detail in each. He can appreciate in a manner beyond his ability to describe a painting or the motion of a dancer, and he can do so on a moonlit night or under a bright sun. Such perceptions are stimulated by patterns of light but are modified by intention and experience. For example, most readers of this page will be conscious of the meanings of the words printed here, not of the lines comprising the letters of each word. However, if this page were examined for printing quality or by someone never exposed to printed English, the opposite would be true.

All of these visual functions and more may come into play in the use of an image communication system and, thus, quantitative models for these

functions would be useful in system design. However, given the current state of scientific knowledge, such models seem impossible. Consider the visual ability to recognize a familiar object or pattern with virtual indifference to wide variations of position, size or shape. Over the past two decades scientists and engineers have attempted to model and mimic this ability for a class of patterns including only alphanumeric. Although this study of "character recognition" was greatly simplified by its severe restrictions on input patterns, success was minimal. Hence, the first task of this research was to identify a subset of visual function for which modelling appeared both possible and useful.

Steps towards limiting modelling possibilities involved both the choice of an experimental technique which would minimize psychological considerations and the selection of an existing model for study. Some of the least understood functions of visual perception are said to involve psychological parameters (e.g. memory, training, intention). In this work those parameters were eliminated from study by asking the following question. "How may one calculate the light pattern perceived given that viewed?" Presumably, the answer to that question is determined by visual neurophysiology which is common to all men at all times. In time the answer may be found by neurophysiologists. The visual neuro-pathway is already known to have a layered structure and coarse descriptions of the functions of the cells in each layer (up to areas 17 and 18 in the cortex) are known. Unfortunately, this approach has not progressed to the point where it can be powerfully related to perceived patterns. No one has any idea what goes on beyond areas 17 and 18. In particular the neurological process consciousness is completely unknown. Thus, if one wants to determine what pattern is perceived when a known light intensity

pattern is viewed, one must display that pattern and ask the viewer what he sees. Conscious response to test stimuli for the purpose of exposing physiological principles is termed "psychophysics" and is the technique used in this research.

The only remaining aspect of technique which affects research objectives is the decision to do detection experiments. Having determined to ask a subject for conscious responses to stimuli, it is crucial to realize that there are many responses which he will be unable to make with accuracy. For example, if an image like that of Fig. 1.1 is displayed with sufficient contrast, a subject will always report the right side to be brighter than the left. However, he will be unable to accurately quantify such features of the image as the luminance of the two halves or the difference in luminance between the two halves. Suppose, on the other hand, that the same image is briefly exchanged for a field of constant luminance and that image contrast is lowered to the point where it is barely distinguishable from the constant field. Suppose further that the subject's task is to respond according to his confidence that he perceived a change when the test image was introduced. This would be a detection experiment. In such experiments the minimum contrast at which a subject can detect a difference is reasoned to be a function of the physiology under study and not of any psychological parameters. Further, the subject's task is one which he can perform with minimum difficulty and maximum accuracy since the uncertainty or noise in his responses is believed to result from noise inherent in the physiological mechanism.

Detection experiments can be performed by subjects and interpreted by experimenters, but can they yield information useful for modelling? The answer is "yes" and is known by example. The name "Frequency Channel

Model" applies to a class of evidence and thought which approach the kind of modelling desired in this research. Chapter 2 discusses this model in detail, but for the purpose of technique selection, it is enough to comment that this model came from and can be pursued with detection experiments.

The previous comments on goal reduction come from a consideration of the "state of the art". Several of the same conclusions might be reached via modeling considerations. First, the Frequency Channel Model incorporates some of the most useful features of linear systems theory. (See section 2.3.) Second, visual perception, even restricted to perceived light patterns, is a highly nonlinear phenomenon and nonlinear systems are typically modelled with small-signal linear models. Limiting study to that of detection constrains system inputs to be perceptually small with the result that they may be small with respect to system nonlinearities and, hence, yield a linear model. Finally, most image communication systems are designed for high fidelity and thus differences between input and output should be perceptually small. Detection experiments of the sort performed here can be described as a study of the properties of distortion which determine its perception when the communicated image is spatially constant. Since the user's visual system is not a function of its input, it is hoped that a model which works for constant images could be extended easily to cover larger classes of images.

For these reasons this research considers detection and in particular the Frequency Channel Model of detection.

1.2. Overview of the Dissertation

In chapter 2 the FCM is discussed, first in terms of the vision research which supports it and second in mathematical terms. Specific conclusions are drawn about what is known and a further test of the model is selected.

Chapter 3 discusses experimental equipment and procedure. Stimuli were generated numerically and displayed on a television monitor. Experiments were computer controlled. The subject's response task, called a "rating" task, is explained.

Chapter 4 describes the experiment used to perform the test of the FCM which was developed in chapter 2. It also gives plots of the resulting data. Experimental stimuli contained either one or two half-field sinusoidal grating patches. Two spatial frequencies, 12.8 cycles per degree and 4.3 cycles per degree , were used. In some two-patch stimuli the patches were at different frequencies. In others they were at the same frequency. Because responses to single patch stimuli were also measured, it was possible to calculate precisely the behavior which should have occurred whenever the two patches of a two-patch stimulus were detected independently. These PSUM calculations are also plotted. Only one conclusion is drawn from the data in this chapter and it relates to the manner in which the data are plotted, not to any model for visual detection.

In chapter 5 the data are examined and conclusions are drawn. Our findings support existing evidence that sinusoids at different frequencies are detected independently. Similarly, we find that two adjacent patches at 4.3 cycles per degree appear to be detected independently. This agrees with existing evidence that individual striations of such gratings are detected independently. Finally, we find that adjacent patches at 12.8 cycles per degree are

detected far more easily than can be explained by the independent detection of each patch. This is taken to mean that the individual striations of sinusoidal gratings at this frequency are not detected independently. Instead, we conclude that there exists some single mechanism which is not only selective for this frequency but also sensitive to several cycles of the grating.

There is one appendix. It contains short descriptions of other experiments performed in the course of this research. These experiments have been relegated to an appendix because they are largely inconclusive. However, three of them repeat the above test for spatial summation at frequency 12.8 \sim /0 but with a somewhat different result. The reader may wish to consider those data together with that of chapter 4.

CHAPTER 2

THE FREQUENCY CHANNEL MODEL

2.1. A Description of the FCM

The name Frequency Channel Model (FCM) applies to a class of pattern detection models which have two concepts in common. The first is that detection occurs as if via several independent parallel mechanisms or "channels" each capable of performing the detection function. The second is that each channel is sensitive to a class of patterns which is localized in the Fourier transform domain.

Figure 2.1 contains a block diagram for the FCM in its simplest form. Recall that in detection experiments the subject's task is to detect a difference between some continuously-viewed background image and a briefly-viewed test image. Any still achromatic image may be represented analytically as a two-dimensional real function, $I(\cdot, \cdot)$. The arguments, say x and y , represent horizontal and vertical distance, in degrees, from the center of the visual field. Images of interest here are restricted to some small, $N^0 \times N^0$, portion of the visual field and hence, each argument ranges through the interval $[-N/2, N/2]$. $I(x, y)$ represents image luminance at the point (x, y) . Thus, the background image is one such function, say $I_B(\cdot, \cdot)$ (It is typically constant, $I_B(x, y) \equiv I_0$), and the test image another, say $I_T(\cdot, \cdot)$. The subject's task may now be described as that of detecting the image $I(\cdot, \cdot)$ where $I(x, y) \triangleq I_T(x, y) - I_B(x, y)$ and it is this image which appears at the input to the block diagram in Fig. 2.1.

In the diagram the input, I , is seen to appear at the input to several parallel horizontal paths. These are the channels and each carries that same input to a detection decision; "1" meaning that detection has occurred,

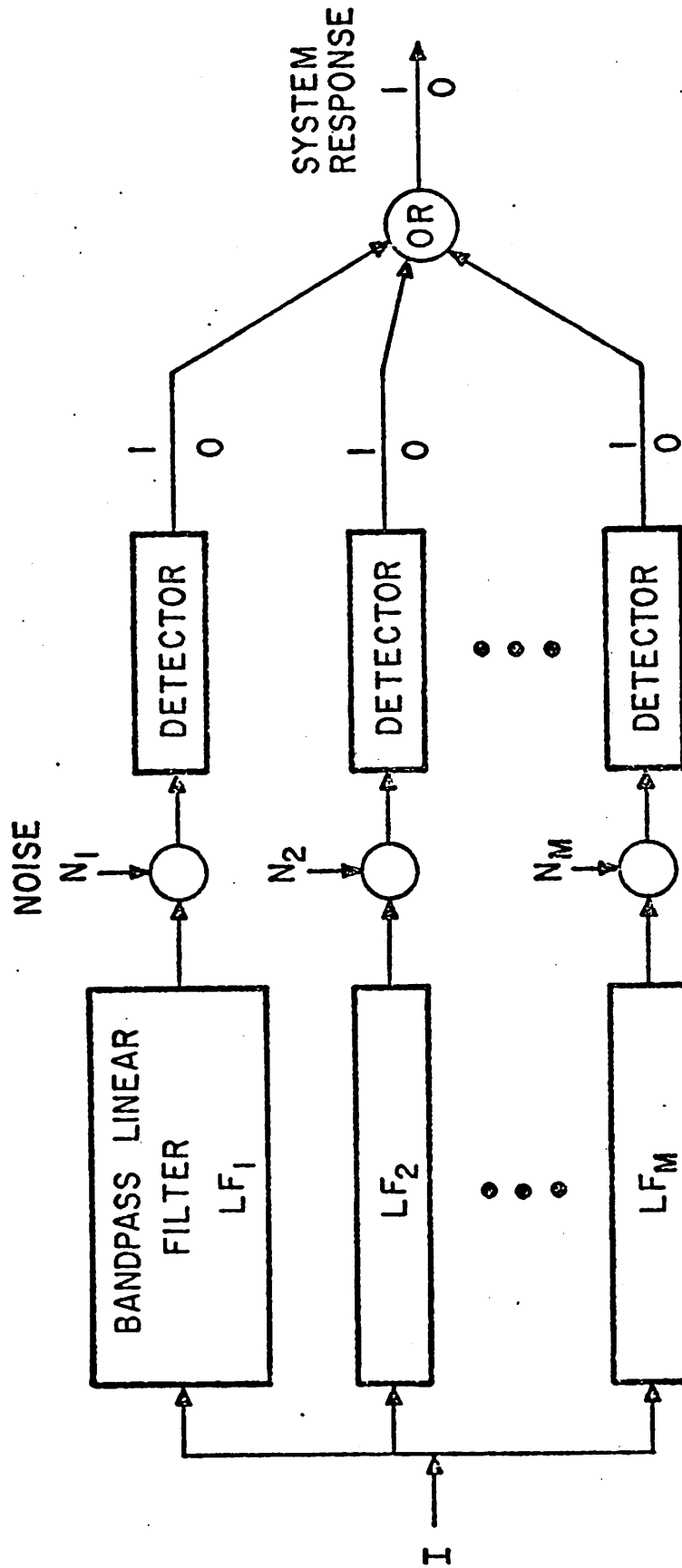


Fig. 2.1. The Frequency Channel Model.

"0" that it has not. Channel outputs are combined with a logical "OR" function, system response being "0" if and only if the same is true for every channel. It is important that noise is introduced in each channel before the detection decision is made. The noise in each channel is assumed independent of the input I and of the noise in all other channels. Hence, a given image may be detected on one trial and not on another. Also, it may be detected by one channel on one trial and by another on another trial. This treatment of the noise in detection renders channels complete and independent detection mechanisms.

The first operation performed by each channel is that of bandpass linear filtering. In order to understand the intended meaning of this crucial portion of the model, certain properties of the Fourier transform must be discussed. (A more complete discussion may be found in Sakrison [3]). Since every image may be represented as a real function on the real plane, each has a two-dimensional Fourier transform. Because each image is defined only on a rectangle, $[-N/2, N/2] \times [-N/2, N/2]$, in the plane, these transforms are Fourier series. Let

$$K = \{j/N : j \text{ is an integer}\}.$$

Then, if we let $i(\cdot, \cdot)$ denote the Fourier transform of $I(\cdot, \cdot)$, it is defined on $K \times K$ and we have

$$i\left(\frac{k}{N}, \frac{l}{N}\right) \triangleq \frac{1}{N} \int_{-N/2}^{N/2} \int_{-N/2}^{N/2} I(x, y) e^{-j\Omega(kx+ly)} dx dy$$

$$I(x, y) = \frac{1}{N} \sum_{k, l=-\infty}^{\infty} i\left(\frac{k}{N}, \frac{l}{N}\right) e^{j\Omega(kx+ly)} \quad (2.1)$$

where $\Omega \triangleq 2\pi/N$ and $j \triangleq \sqrt{-1}$. Because I is real, i is complex symmetric.

That is,

$$i\left(\frac{-k}{N}, \frac{-l}{N}\right) = i^* \left(\frac{k}{N}, \frac{l}{N}\right) \quad \left(\frac{k}{N}, \frac{l}{N}\right) \in K \times K.$$

This property has an important consequence. Consider the sum of the $(k/N, l/N)$ and $(-k/N, -l/N)$ terms in Eq. 2.1.

$$\begin{aligned} & i\left(\frac{k}{N}, \frac{l}{N}\right) \left(\frac{1}{N}\right) e^{j\Omega(kx+ly)} + i\left(\frac{-k}{N}, \frac{-l}{N}\right) \left(\frac{1}{N}\right) e^{j\Omega(-kx-ly)} \\ &= i\left(\frac{k}{N}, \frac{l}{N}\right) \left(\frac{1}{N}\right) e^{j\Omega(kx+ly)} + i^* \left(\frac{k}{N}, \frac{l}{N}\right) \left(\frac{1}{N}\right) e^{-j\Omega(kx+ly)} \\ &= R_{k\ell} \cos[(kx+ly) \Omega + \phi_{k\ell}] \end{aligned} \quad (2.2)$$

where $R_{k\ell} \triangleq \frac{2}{N} \|i\left(\frac{k}{N}, \frac{l}{N}\right)\|$

$$= \frac{2}{N} \sqrt{\text{Re}^2 \left[i\left(\frac{k}{N}, \frac{l}{N}\right) \right] + \text{Im}^2 \left[i\left(\frac{k}{N}, \frac{l}{N}\right) \right]}$$

and $\phi_{k\ell} \triangleq \arctan[\text{Im}(i\left(\frac{k}{N}, \frac{l}{N}\right)) / \text{Re}(i\left(\frac{k}{N}, \frac{l}{N}\right))]$.

Imagine the image which results from fixing k and l in Eq. 2.2 while varying x and y . If one moves along the lines

$$kx + ly = c \quad c \in \left(-\frac{N}{\sqrt{2}}, \frac{N}{\sqrt{2}}\right)$$

in the visual plane, the value of Eq. 2.2 remains constant. If one moves perpendicular to such a line, that is at angle

$$\theta_{k\ell} \triangleq \arctan\left(\frac{l}{k}\right), \quad (2.3)$$

the image intensity varies sinusoidally at a frequency

$$f_{k\ell} \triangleq \frac{1}{N} \sqrt{\ell^2 + k^2} \quad \text{cycles per degree } (\sim/\circ).$$

(Note that f and θ are the radius and angle of the polar representation of the domain of $i(\cdot, \cdot)$.) Such an image is called a sinusoidal grating with frequency f , orientation θ , amplitude R and phase ϕ .

It is now possible to explain the bandpass linear filters in Fig. 2.1. Substituting Eq. 2.2 into Eq. 2.1 yields

$$\begin{aligned} I(x,y) = & \sum_{k=1}^{\infty} \sum_{\ell=-\infty}^{\infty} R_{k\ell} \cos[(kx+\ell y) \Omega + \phi_{k\ell}] \\ & + \sum_{\ell=1}^{\infty} R_{0\ell} \cos(\ell y \Omega + \phi_{0\ell}) + \left(\frac{1}{N}\right) i(0,0). \end{aligned} \quad (2.4)$$

This shows that any image may be considered to be the sum of many sinusoidal grating images. Roughly speaking, the FCM says that the visual system breaks down that sum, making an independent decision on each component. More particularly, each channel has associated with it a single f and θ and is believed sensitive only to images (e.g. sinusoidal image components) which are similar to sinusoidal gratings at that f and θ . However, just what kind of similarity is required is not completely known. As is discussed in section 2.4, this research probes this question. What is known is that gratings which differ greatly in frequency or orientation from the f and θ for a particular channel will not be detected by that channel. This fact is the motivation for and meaning of the linear filters in Fig. 2.1. Each filter is bandlimited in both the f (radial) and θ (angular) dimensions and, thus, passes only image content which is similar in frequency and orientation to the filter's centerpoint.

2.2. Evidence Supporting the FCM

Campbell and Robson (1964,1968)

The earliest form of the FCM was proposed by Campbell and Robson [4,5]. Their experiments indicated that, for a wide range of spatial frequencies, the detectability of a sinusoidal grating is not affected either by the presence of subthreshold gratings at frequencies at least twice that of the test or by a suprathreshold background grating at a frequency one-third that of the test.

These investigators used a "self-setting" experimental technique. The subject viewed an image which consisted of an always-present background image plus a zero-mean stimulus, the "I" of Fig. 2.1, which was switched on and off at a rate of .5 Hz. The subject's task was to adjust the amplitude or contrast of the stimulus to the level where it was judged "barely detectable." Using this technique they measured the threshold contrast of sine, square, rectangular and saw-tooth gratings against a constant background. For most frequencies of the non-sinusoidal stimuli they found that detection occurred as if only the fundamental (lowest frequency) component were present (see Eq. 2.4).

In a second experiment the background contained a suprathreshold sinusoidal grating at some frequency f . The stimulus consisted of all higher harmonics (sinusoidal grating components at frequencies above f) of a square wave grating at frequency f . The subject adjusted one knob which controlled the contrast of both background and stimulus (so that when the stimulus was present the total image was always a square wave) until the stimulus was barely detectable. Once more they found that, for a wide range of frequencies f , the stimulus was detected as if only its lowest frequency ($3f$) component were present.

Campbell and Robson [5] concluded that this behavior could be modelled with "linearly operating independent mechanisms selectively sensitive to limited ranges of spatial frequencies." This conclusion corresponds to the channel structure of the FCM and to the radially bandpass nature of the filters in Fig. 2.1.

Sachs, Nachmias and Robson (1971)

Sachs, Nachmias and Robson [6] performed an experiment which confirmed the conclusion of Campbell and Robson and probed the role of noise in the model. In order to do so, they used a technique which focused on the shape of psychometric functions.

In this experiment the background image was always constant and stimuli were of the form

$$I(x,y) = L_0 [m \cos(2\pi f x + \phi) + m' \cos(2\pi f' x + \phi')] \quad (2.5)$$

A subject would initiate each trial by pressing a switch whereupon the stimulus would be added to the background for a brief time. The subject's response task was to answer "yes" if he detected any change when the stimulus was presented, "no" if he saw none. This approach yields detectability data in the form of psychometric functions. That is, the probability of detection is plotted as a function of stimulus contrast as in Fig. 2.2.

The standard definition for the contrast, C , of an image is

$$C \triangleq (L_{\max} - L_{\min}) / 2 L_{\text{avg}}$$

where L_{\max} , L_{\min} and L_{avg} are image maximum, minimum and average luminances. When applied to a zero-mean image component (e.g. the sinusoidal components

of Eq. 2.4), the word "contrast" means the same calculation but in this case L_{\max} and L_{\min} are those for the component and L_{avg} is that for the composite image. For the images of Sachs et al. $L_{\text{avg}} = L_0$ and thus, Eq. 2.5 shows that the contrast of the frequency f component is m and that of the f' component is m' .

In any single experimental session ϕ , ϕ' , f and f' (Eq. 2.5) were fixed. On some trials the frequency f component was presented alone ($m'=0$) at various contrasts. On randomly interleaved trials m' was set to a constant positive value and m was varied again. This procedure yielded a pair of psychometric functions both plotting "proportion seen" versus m . In the case where $m'=0$ the function and stimulus were called "simple." When m' was positive they were called "complex" (Fig. 2.2).

Sachs et al. observed that if a model like that of Fig. 2.1 applied, and if each component of a complex image were processed only by its own channel, then the response to the complex image should be the probability summation of the responses to the two components presented by themselves. Probability summation is explained in detail in section 2.4. Here it is enough to know that when it occurs the two psychometric functions from a single session will be related in a specific, simple way. Figure 2.2 shows two such pairs. In each case the complex psychometric function has been fitted with a curve calculated from the simple curve according to the probability summation assumption. We see that for $f' = 0.93$ the fit is good, but for $f' = 1.4$ it is poor. Thus, the first case could result from probability summation and the second could not.

In general their data contradicted probability summation only when f' was close to f . This can be seen as a two-part result. First, the viability of a probability summation model allows the placement of system

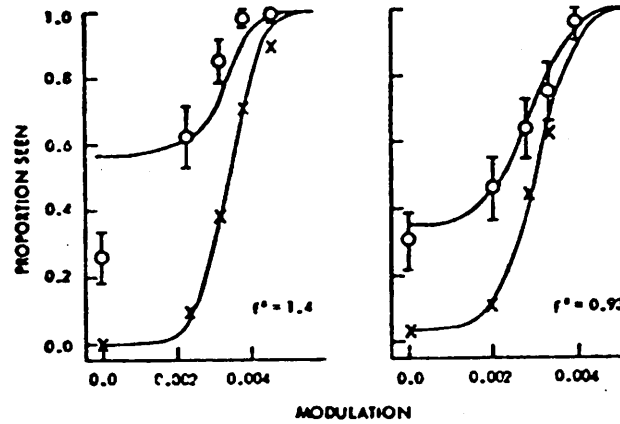


Fig. 2.2. Simple (X's) and complex (O's) psychometric functions for $f = 2.8$ and $f' = 1.4$ and 0.93 -/0. Simple functions were fit with solid curves of pre-determined shape. Complex functions were fit with curves calculated from the simple functions using a probability summation assumption. (Taken from Fig. 10 of [6].)

noise and the detection function within individual channels (Fig 2.1).
 Second, the fact that channel-like behavior occurs if and only if components differ significantly in frequency supports the bandpass characteristic proposed by Campbell and Robson.

Kulikowski, Abadi and King-Smith (1973)

At this point the only aspect of Fig. 2.1 which remains unsupported is the angular selectivity or θ -dimension bandpass characteristic of the linear filters. This was demonstrated by Kulikowski, Abadi and King-Smith [7].

Their technique, called "subthreshold summation," can be viewed as a synthesis of the two previous techniques. Since they required only a single detectability figure for each test condition, a self-setting technique was used. However, like Sachs et al., their conclusions derived from a consideration of how the presence of one image component affected the detectability of another.

In these experiments the stimulus I remained unchanged throughout each session. The subject's task on each trial was to adjust stimulus contrast to threshold. What varied from trial to trial was the background. On some trials the background was constant. On others a sinusoidal grating was added. The contrast, C_b , of these background gratings was always set to be barely subthreshold -- the subject never perceived them. Since the subject always adjusted the same stimulus to threshold, it was reasoned that the same channel was always accomplishing detection. Usually they found that threshold contrast in the presence of a subthreshold grating, C_t , was different from that on the blank background, C_{ot} . Assuming that the detection process was linear, the sensitivity, S , of the channel under study to the subthreshold background grating was calculated from this difference in the following manner (Kulikowski and King-Smith [8]).

$$S = (C_{ot} - C_t) / C_{ot} \cdot C_b$$

Data were taken for the case where stimulus and background gratings were both sinusoidal at frequency 10 \sim /0 and also for the case where both were sinusoids at 5 \sim /0. In each case the angle, θ in Eq. 2.3, between stimulus and background was varied from trial to trial. Their finding was that the sensitivity of both the 10 and 5 \sim /0 channels to the background gratings decreased monotonically as θ increased. For both channels

the sensitivity reached one-half maximum at a rotation of 3° . This result indicates a very narrow angular bandpass characteristic for the filters of Fig. 2.1.

Of course, almost any experimental result will admit more than one model. In that sense it may be said that the techniques and results discussed in this section are inconclusive. For example, Mostafavi and Sakrison [9] have proposed a version of the FCM in which specific assumptions are made about the structure of a channel's detection mechanism. In that model the angular selectivity mentioned above results from both the filter and the detection mechanism. However, models are chosen to serve the purposes of the user as much as they are to explain the data. This section shows that the FCM of section 2.1 gives structure to existing experimental results. The next section shows that it serves modelling objectives. The usefulness of this model appears in section 2.4 where it helps us decide what experiment to perform.

2.3. The FCM as a Mathematical Model

It was explained in Chapter 1 that the primary motivation in this research is the need for a mathematical model of human visual perception. In this section we comment on the potential of the FCM to fill that need.

It is first necessary to observe that the FCM is very incomplete. What is needed is a model which can quantitatively predict visual response to an arbitrary member of a large class of stimuli. As it exists today, the FCM does little more than give a qualitative explanation for measured responses to a relatively small class of stimuli. Yet the FCM has the structure of a mathematical model and there are reasons for pursuing this particular structure.

Some models are better than others. The best ones are the most useful ones. Two aspects which affect a model's usefulness are its generality and its simplicity. We discuss the structure of the FCM in these terms.

Linear systems theory provides excellent models for many physical systems. For example, the input/output characteristics of a linear amplifier may be completely determined by measuring its transfer function. It operates as if it processes "each frequency component" of an input independently in accordance with the transfer function and then outputs the sum of the processed components. This model is general because it is accurate, without change to the transfer function, for all inputs to which the amplifier's response is linear. The model is simple because a transfer function is easy to measure and to manipulate analytically.

The visual system is highly nonlinear. One example of this fact was demonstrated by Sachs, Nachmias and Robson [6] and again in the present experiment. A stimulus may contain two components each of which contributes to its detection. Yet, the response to the composite cannot always be known from a knowledge of the response to each component. Because it models a nonlinear system, the FCM is itself nonlinear. Its nonlinearity results both from the quantized nature of its outputs and from its channel structure. Nonetheless, this model offers some of the important advantages of linear models.

The most important aspect of the FCM is its channel structure. Because each channel performs only a portion of the overall detection task, each is simpler than the overall system. Presumably the characteristics of each channel can be determined experimentally with the use of specialized stimuli. (For an example of such a study see Mostafavi and Sakrison [9].)

Thereafter the response to an arbitrary stimulus may be calculated by probabilistically summing the calculated responses of each channel. Thus, whereas a linear system decomposes an input according to frequency, the FCM decomposes an input according to channel characteristics. The result in each case is simplicity. One complex input/output calculation is reduced to several simple ones.

Any channel model offers this potential for simplicity. In fact, channels different from those of the FCM have been proposed and some are discussed in the next section. Yet the FCM may be more useful than the apparent alternatives. It proposes that each channel operates within a limited area of the frequency domain. This offers simplicity because the Fourier transform is a particularly manipulable piece of mathematics. The FCM offers generality because every possible stimulus has a unique frequency domain representation. Thus, a set of channels which spans the frequency domain necessarily spans the class of all inputs.

2.4. Other Models and the Present Test of the FCM

At this point we are in the happy circumstance that a model indicated by psychophysical research suits our purposes. In this section we observe that the evidence cited in section 2.2 admits but does not mandate the FCM. In particular, if one assumes that all detection behavior can be modelled with some finite set of independent channels and that this set is unique -- call this the Channel Model -- it remains to be shown that all or even any of those channels are frequency channels.

Probability Summation

As stated in section 2.2, the phenomenon of probability summation is essential to the reasoning of Sachs, Nachmias and Robson [6]. On the

strength of their work we conclude that the visual system can be modelled with independent channels. However, the following analysis of probability summation shows that one cannot conclude from that result that the activity of any single channel has been isolated.

Assume that the Channel Model contains M independent channels, each with its own detection mechanism and independent noise source. Let

$P(N/I) \triangleq$ the probability that a subject will respond "no" when stimulus I is viewed briefly against a blank background.

For $1 \leq j \leq M$ let

$P_j(N/I) \triangleq$ the probability that I is not detected by channel j .

Then the independence of the channels implies

$$P(N/I) = \prod_{j=1}^M P_j(N/I).$$

This is probability summation. Its effect on system behavior can be seen by example. Let $I = \alpha_1 I_1 + \alpha_2 I_2$ where I_1 and I_2 are any stimuli with the property that only channel 1 is sensitive to I_1 and only channel 2 is sensitive to I_2 . Then

$$P_j(N/\alpha_1 I_1 + \alpha_2 I_2) = \begin{cases} P_j(N/\alpha_j I_j) & j \leq 2 \\ P_j(N/\text{blank}) & j > 2 \end{cases}$$

$$\text{and } P(N/\alpha_1 I_1 + \alpha_2 I_2) = P_1(N/\alpha_1 I_1) P_2(N/\alpha_2 I_2) \prod_{j=3}^M P_j(N/\text{blank}). \quad (2.6)$$

Note that $\alpha_1 I_1 + \alpha_2 I_2$ is more detectable (more often detected) than either $\alpha_1 I_1$ or $\alpha_2 I_2$ even though neither affects the detection of the other.

Now it is possible to describe the test for independence used by Sachs et al. (See section 2.2). Let I_1 and I_2 represent, respectively,

their gratings at f and f' . Let α_1 and α_2 represent m and m' . Then, under their independent channels hypothesis, Eq. (2.6) holds. Viewing Eq. (2.6) as a function of α_1 with $\alpha_2 > 0$ constant it is an expression for their complex psychometric function. (Strictly speaking, the psychometric function plots the probability of detection versus α_1 . However, the probability of detection always equals 1 minus the probability of no detection so it is enough to consider Eq. (2.6).) Similarly, their simple psychometric function ($\alpha_2 = m' = 0$) is given by

$$P(N/\alpha_1 I_1) = P_1(N/\alpha_1 I_1) \prod_{j=2}^M P_j(N/\text{blank}). \quad (2.7)$$

Equations (2.6) and (2.7) may be combined to yield the following.

$$P(N/\alpha_1 I_1 + \alpha_2 I_2) = P(N/\alpha_1 I_1) \left[\frac{P_2(N/\alpha_2 I_2)}{P_2(N/\text{blank})} \right] \quad (2.8)$$

Note that the term inside the square brackets is independent of α_1 . Thus, the independent channels assumption implies that the compliment of the complex psychometric function is a scaled version of the simple one. This was their test for independence. When they found a constant c such that

$$P(N/\alpha_1 I_1 + \alpha_2 I_2) = cP(N/\alpha_1 I_1) \quad (2.9)$$

for all tested values of α_1 , they concluded that the data was consistent with the independent channels hypothesis. (The value of c was chosen for best fit in Eq. (2.9). In the experiment of chapter 4 c is chosen according to Eq. (2.8).) When no such c existed, they rejected the independence possibility.

In the above calculations it was assumed that each image component stimulated only one channel. Suppose now that I_1 stimulates only channels

1 through M_1 and that I_2 stimulates only channels M_1+1 through M_2 . Then

$$\begin{aligned}
 P(N/\alpha_1 I_1) &= \prod_{j=1}^{M_1} P_j(N/\alpha_1 I_1) \prod_{j=M_1+1}^M P_j(N/\text{blank}) \\
 P(N/\alpha_1 I_1 + \alpha_2 I_2) &= \prod_{j=1}^{M_1} P_j(N/\alpha_1 I_1) \prod_{j=M_1+1}^{M_2} P_j(N/\alpha_2 I_2) \\
 &\quad \prod_{j=M_2+1}^M P_j(N/\text{blank}) \\
 P(N/\alpha_1 I_1 + \alpha_2 I_2) &= P(N/\alpha_1 I_1) \prod_{j=M_1+1}^{M_2} \frac{P_j(N/\alpha_2 I_2)}{P_j(N/\text{blank})} \quad (2.10)
 \end{aligned}$$

Once again simple and complex psychometric functions are related by a factor which is independent of α_1 . This shows that this test for independence cannot distinguish between the activity of single channels and that of disjoint groups of channels. Thus, if we assume the existence of the Channel Model, we must conclude that the visual mechanisms which detect sinusoidal gratings may not be single channels.

Other Types of Channels

In the FCM all image activity at a particular f and θ is assumed to be processed by a single channel. One implication of this assumption is that a single frequency channel has broad spatial extent. Robson [10] measured the detectability of a sinusoidal grating as a function of the number of cycles present and found it continued to increase up to widths of twenty cycles and more, regardless of grating frequency.

In the FCM all channels are frequency channels. Thus, if the FCM and the channel Model (CM) are the same model, then all channels have broad spatial extent. However, to our knowledge, no previous evidence

shows that any single channel is spatially broad. On the other hand, Kulikowski and King-Smith [8] have proposed the existence of at least two types of channels which have limited spatial extent. They call one of these the "threshold line detector." The optimum stimulus for that detector is given in Fig. 2.3. Its appearance is somewhat similar to that of 1.5 cycles of a sinusoidal grating at 5 cycles/degree. In fact, if channels like that are located at many positions within the visual field, then the detectability of a 5 -/0 sinusoidal grating might be explained by the probabilistically summed responses of several, each reacting to 1.5 cycles. Kulikowski and King-Smith pursued this possibility in another paper [11]. There they proposed that evidence like that of section 2.2 regarding the detection of sinusoidal gratings might be explained by the existence of line detectors of various widths.

These two papers affect the status of the FCM in two ways. First, if line detectors (or any channels other than frequency channels) are demonstrably single channels, then they belong in the CM. This would mean that the CM contained channels not found in the FCM and, thus, that the FCM was an incomplete model. Second, if the evidence for the FCM can be explained with line detector channels (i.e. without the assumption of frequency channels), then one is lead to assume that no frequency channels exist and that all that remains of the FCM is its channel structure.

The Present Test

We have emphasized one essential difference between the FCM and alternatives represented by the work of Kulikowski and King-Smith. It is the spatial breadth of a single channel. The intent of the present

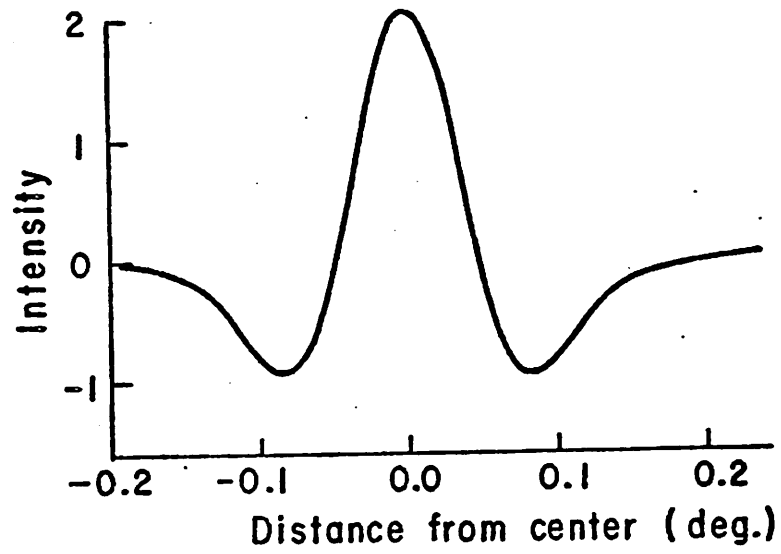


Fig. 2.3. The threshold line detector. This detector is believed to be selectively sensitive to stimuli with this crosssection.

experiment is to determine whether or not in the detection of a sinusoidal grating a single channel has spatial breadth greater than 1.5 cycles.

In order to do so, we measured psychometric functions for stimuli which contained half-field sinusoidal patches either on the left side, the right side or both sides of the center of the visual field. Patches at two different frequencies were used and, when two of the same frequency were presented together, there was a space of either 0.5 cycle or 1.5 cycles between them. Reasoning as Sachs, Nachmias and Robson did, we could call one-patch stimuli "simple" and two-patch stimuli "complex." Then, because components of the complex stimuli were spatially separate, the Kulikowski and King-Smith model predicts that the relationship between simple and complex psychometric functions should correspond to probability summation (Eq. (2.8)). When this occurred, we concluded that the concept of spatially narrow channels had been supported. When it did not occur, we concluded that at least one single channel had enough spatial breadth to overlap portions of both patches.

CHAPTER 3

METHODS

3.1. Technique

The general form of a detection experiment has been described. A subject attempts to detect a stimulus $I(\cdot, \cdot)$ when it is added to a background image $I_B(\cdot, \cdot)$. In this section the specific procedure used in the present experiment is described and the subject's response task, called a "rating" task, is explained.

Procedure

The basic unit of experimental procedure was the trial. One day's work for a single subject, an experimental session, consisted of 4 rounds of 100 trials each. All sessions were performed under computer control. Each trial consisted of the following steps.

1. The subject sat, head motionless, fixating a small dark spot in the center of a constant luminance ($I_B(x,y) \cong 860 \text{ cd/m}^2$) TV screen.
2. The computer pulsed a buzzer to indicate that the trial could begin.
3. When he was ready, the subject activated an electronic switch which added the stimulus to the background for .54 seconds.
4. By pressing one of several buttons, the subject responded according to his confidence that he had detected a change on the screen when the stimulus was added.
5. The computer recorded the response and then rang a bell if the stimulus had been a blank ($I(x,y) \cong 0$).
6. The computer selected a stimulus for the next trial and pulsed the buzzer to start the sequence over again.

Before each round the subject reacclimated himself to the task by performing 10 or more practice trials. When all 100 trials for a given round had been completed, the computer broke the cycle and the subject

rested for approximately 2-5 minutes. Each round contained the same set of stimulus conditions but their order was varied from round to round with the use of a random number generating subroutine. At the end of the fourth and final round of each session the day's data was punched onto cards.

The subject was provided with 8 response buttons labelled with the numbers 1 through 8. Buttons 1 through 5 corresponded to the responses explained in the next subsection. Button 6 meant "I blinked" and caused the trial to be repeated at a pseudo-random position in the remainder of the round. Buttons 7 and 8 were used for program control instructions such as "I am done practicing. Start the next round."

Each complete set of data, that is each set of curves in chapter 4, corresponds to 15 four-round sessions or $4 \times 15 = 60$ responses to each of the 100 stimulus conditions. Each session took 35 to 45 minutes and subjects were limited to one session per day. All subjects were required to perform practice sessions (at least 5, sometimes many more) until it was felt that their responses were consistent from day to day. Once this consistency was achieved, subjects were required to work 5 out of every 7 days and the next 15 sessions, regardless of day to day consistency, comprised the final set of data. This process was repeated 5 times, twice each with subjects DDS and MCH, once with subject CDJ.

The subjects used either had hemotropic vision or vision correctable to 20/20 with glasses. Binocular vision with natural pupils was used throughout. One subject, MCH, was the experimenter. Subject DDS was a university lab technician with approximately two years of experience as a subject in similar experiments but with no knowledge of experimental objectives. The third subject (CDJ) was a graduate student in electrical

engineering. He had approximately three months' experience as a subject and a rough understanding of experimental objectives. All subjects were approximately 30 years old.

As was mentioned above, some of the stimuli were blank. There were 20 such trials per round and they were included for three reasons. First, they serve to control guessing. A subject might respond positively (i.e. "Yes, I saw it.") on every trial, whether he saw something or not, if he knew that every trial contained a nonzero stimulus. By recording responses to blanks and by ringing a bell after each blank trial, subjects are given ample feedback with which to control such guessing. Second, blanks provide a useful aid to the subject in establishing his threshold criteria. The subject's task is a detection task. He is to respond positively whenever he perceives any change on the screen during the stimulus presentation time, whether or not he recognizes his perception as one of the possible stimuli. However, both the display equipment and the visual system itself contain enough noise that some change is almost always perceived. Even when a subject is not guessing, positive responses to blanks result from this noise. The subject must therefore learn to respond positively only to changes which he considers more likely to have resulted from nonzero stimuli than from blanks. The criterion he used to make this discrimination is called his threshold criterion. Frequent presentation of blanks and immediate feedback on each (the bell) were considered important for the creation and maintenance of this criterion. Third, the probability of a negative response to a blank stimulus must be known for the calculations of section 3.2.

Subject's Response Task - Rating

It was just explained that feedback on blank trials aids the subject in establishing a threshold criterion. The implication is, of course, that the subject has some control over this criterion. We all know this to be true from personal experience. Certainly, one can easily adopt a criterion so conservative that he never responds "yes" to a blank, but he will then respond "no" to many stimuli which he has good confidence he has seen. Conversely, one can choose to respond "yes" to almost any sensation, but then the average response to blanks will be virtually as strong as that to large stimuli. This ability to adjust threshold criteria has been studied experimentally (Swets [12]). It was found that subjects are able to adopt an appropriate criterion for any desired false alarm rate (probability of a positive response to a blank).

The rating task requires that the subject employ several criteria at once. The task of the present experiment provides an illustrative example. Suppose that all sensations can be ordered in intensity. Then they may be mapped into the real line. Any threshold criterion is a point on that line. Sensations which are mapped to points above the criterion point are detected. Those mapped to points below the criterion are not detected (Fig. 3.1a). Using this model an adjustment of the criterion corresponds to lateral movement of the threshold point on the sensation axis. Now, suppose that the subject is required to select four different criteria at once. He may then compare each sensation with all four criteria, making four responses on each trial. For example, a weak stimulus (labelled "typical sensation" in Fig. 3.1b) might evoke the response "'Yes' on criterion 1, 'no' on criteria 2 through 4." Response

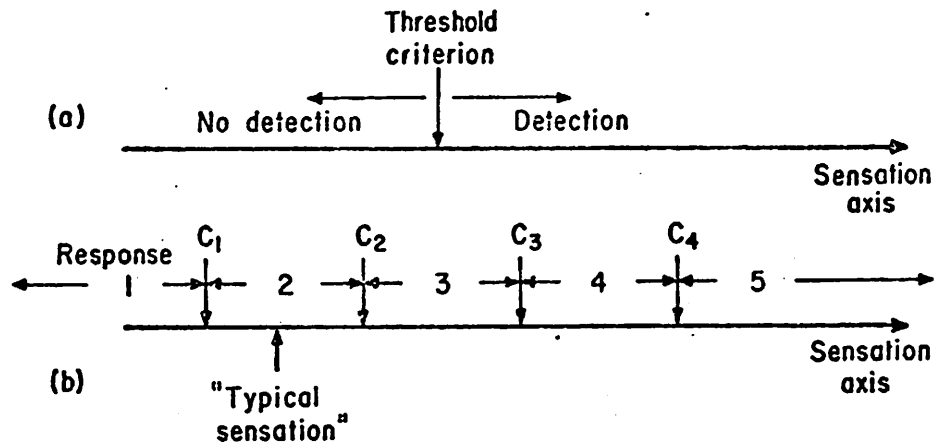


Fig. 3.1. Two types of subject response tasks in detection experiments.

a) Single threshold detection.

b) Four thresholds (C_1 through C_4) and the resulting response regions (1 through 5) used in the rating task.

language may be simplified. In Fig. 3.1b the four criteria are labelled C_1 through C_4 . They divide the sensation axis into 5 non-overlapping regions. Therefore, the subject may unambiguously describe the relationship of his sensation to his criteria by responding with the label of the appropriate region. In the present experiment the numbers 1 through 5 were chosen as labels.

As can be seen from Fig. 3.1b, the larger the number which a subject responds the larger was his sensation. This phenomenon is the source of the name "rating" for this technique. It is, however, important to observe that the response numbers are only labels. As far as the subject's task is concerned the letters A through E could have been used. For this reason it is incorrect to consider subject responses to be a quantification of his sensation. For example, the response "4" does not indicate a sensation which is twice as large as those which result in the response "2". Nonetheless, in this experiment the average of all responses to a given stimulus was taken as the measure of the subject's sensitivity to that stimulus. That this interpretation of the data is justified is a result of the experiment and is explained in chapter 4.

3.2. The Probability Summation Calculation

Sections 2.2 and 2.4 explain how Sachs, Nachmias and Robson used a probability summation test to determine whether or not the components of their complex stimuli were detected by different channels. The present experiment uses a very similar test. However, they collected simple yes/no detection data. The calculation of probability summation predicted behavior is more complex for rating data.

We assume that we have rating data for blanks and for two non-blank

stimuli, I_1 and I_2 . We wish to calculate what the rating data should be for the composite stimulus, I_1+I_2 , when probability summation applies (i.e. when the two components are detected by disjoint groups of channels). The essence of the calculation is Eq. (2.10). However, because the rating task involves four thresholds, that equation must here be applied four times.

Following the notation of section 2.4, assume that there are M channels and that I_1 stimulates channels 1 through M_1 and I_2 stimulates channels M_1+1 through M_2 . Let $q \in \{1,2,3,4\}$ and

$P^q(N/I) \triangleq$ the probability that threshold criterion q (C_q of Fig. 3.1b) is not exceeded when I is viewed.

Because each channel is assumed to be a complete and independent detection mechanism, all four rating thresholds must be used by each and we may write

$P_j^q(N/I) \triangleq$ the probability that threshold q is not exceeded in channel j when I is viewed.

Using this notation, the derivation of Eq. (2.10) yields

$$P^q(N/I_1+I_2) = P^q(N/I_2) \prod_{j=1}^{M_1} \frac{P_j^q(N/I_1)}{P_j^q(N/\text{blank})} \quad (3.1)$$

Now, observe that

$$P^q(N/I_1) = \prod_{j=1}^{M_1} P_j^q(N/I_1) \prod_{j=M_1+1}^M P_j^q(N/\text{blank})$$

and

$$P^q(N/\text{blank}) = \prod_{j=1}^M P_j^q(N/\text{blank}).$$

Therefore,

$$\frac{P^q(N/I_1)}{P^q(N/\text{blank})} = \prod_{j=1}^{M_1} \frac{P_j^q(N/I_1)}{P_j^q(N/\text{blank})}.$$

Substituting this in Eq. (3.1) yields

$$P^q(N/I_1+I_2) = P^q(N/I_2) \left[\frac{P^q(N/I_1)}{P^q(N/\text{blank})} \right]. \quad (3.2)$$

This is the probability summation calculation for the q th threshold. All three quantities on the right-hand side are known from the data in the following manner.

$$P^q(N/I) \triangleq (\text{number of responses to } I \text{ which were } \leq q) / (\text{total number of responses to } I). \quad (3.3)$$

All that remains is to use Eq. (3.2) to calculate the probability summation average response, $A(I_1+I_2)$. For $r \in \{1,2,3,4,5\}$ let

$P(r/I) \triangleq$ the probability of response r given that the stimulus is I .

Then

$$A(I_1+I_2) = \sum_{r=1}^5 rP(r/I_1+I_2)$$

and we need only calculate each $P(r/I_1+I_2)$. But (see Eq. (3.3))

$$P(r/I) = \begin{cases} P^r(N/I) & \text{if } r = 1 \\ P^r(N/I) - P^{(r-1)}(N/I) & \text{if } r \in \{2,3,4\} \\ 1 - P^{(r-1)}(N/I) & \text{if } r = 5. \end{cases}$$

Thus, if we let $I = I_1+I_2$, we see that Eq. (3.2) allows us to solve for each $P(r/I_1+I_2)$ from the data.

3.3. Equipment

Image Creation

All images were constructed numerically on an IBM model 1800 computer and stored in standard television format on a video disk. Numerical representation of each image was on a 512x512 point raster with 8 bit precision at each point.

Experimental Execution Equipment

Figure 3.2 contains a schematic of the equipment used to perform the experiment. The functions of the buzzer, bell, electronic switch, and subject response buttons were explained in section 3.1. The uses of other pieces of equipment are explained below.

Circled "plus" signs: These were impedance-matched, passive networks which outputted the halved sum of two video inputs.

Attenuators 1 and 2: These were impedance-matched, passive networks and were computer controlled via relays. Each could be set to yield any of the attenuations $\{-31, -32, \dots -72, -73\}$ dB where

$$(\text{Attenuation in dB}) = 20 \log_{10} (\text{contrast}). \quad (3.4)$$

"DC Block" circuits: All three outputs of the video disk were non-negative video signals. Since outputs 2 and 3 were used to form the stimulus $I(\cdot, \cdot)$, they were required to be zero mean. The DC block circuits high-pass filtered the video portions of these signals, blocking only the average value of each.

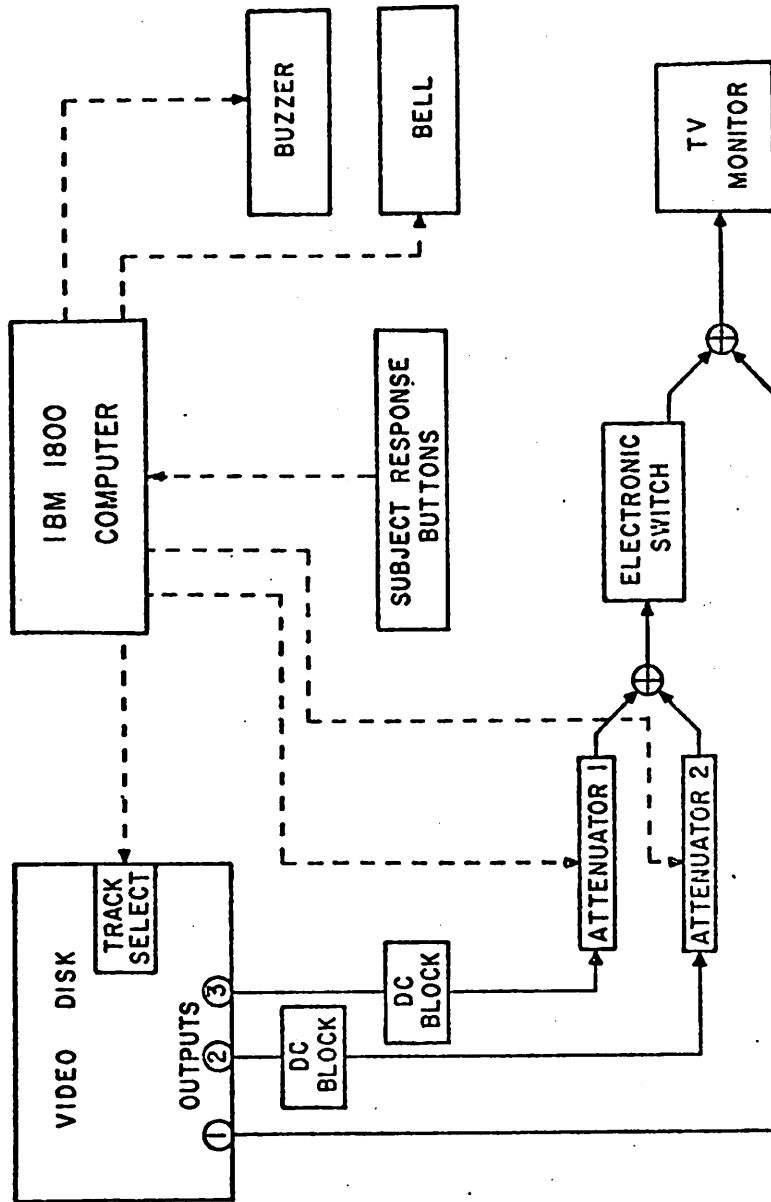


Fig. 3.2. Experimental equipment.

TV Monitor: Images were displayed on an ordinary black and white television with a pale blue (P4) phosphor. The background luminance (860 cd/m^2) was roughly in the middle of its output range. The TV screen subtended approximately $4^\circ \times 4^\circ$ of the subject's visual field. It was surrounded by a 81 cm x 111 cm piece of cardboard with approximately the same color and luminance as the background image. The screen was located just behind a rectangular opening in the cardboard which subtended 3 degrees and 10 minutes vertically and 3 degrees and 36 minutes horizontally in the subject's visual field.

Video Disk: The device used for image storage and retrieval was a video disk. It contained 105 image tracks each of which held 3 independent video signals. When a track was selected, its 3 video signals appeared simultaneously and well-synched at the outputs labelled 1, 2, and 3 in Fig. 3.2.

The Video Path: Output 1 of the video disk always contained the background image and, as the figure shows, was continuously displayed. Outputs 2 and 3 contained stimulus components. The amplitude of each of these signals (and hence the contrast of the corresponding stimulus component - see the discussion of Eq. (2.5)) was controlled with one of the attenuators before they were summed. The composite stimulus fed through the normally-open electronic switch so that the signals of outputs 2 and 3 were only viewed when the subject activated the switch.

IBM 1800 Computer: The computer was given a list of all stimulus conditions. It cycled through this list once each round. Each list entry contained a track number, an attenuation setting for signal number

2, and an attenuation for signal 3. For example, list entries numbered 41 and 42 might be as in table 3.1.

Table 3.1.

<u>STIMULUS NUMBER</u>	<u>VIDEO DISK TRACK</u>	<u>Attenuator 1</u>	<u>Attenuator 2</u>
41	61	-73	-40
42	61	-73	-43

Then for both stimuli, channel 2 contributes nothing and the pattern is that of channel 3 of track 61. However, this pattern appears at a lower contrast in stimulus 42 than in stimulus 41. Such single-pattern stimuli are called "simple." If the third-column entries were both "-48," two-pattern or "complex" stimuli would result.

Using this list, the computer set up each trial by selecting the appropriate video disk track, setting attenuators 1 and 2, and pulsing the buzzer. When the subject responded, the computer recorded the response and rang the bell if the last trial was a blank. It then pseudo-randomly selected a list entry for the next trial. When the subject responded "I blinked" (button number 6), that stimulus condition was returned to the list before the next selection. Therefore, because each selection from the list was made pseudo-randomly, the subject was never able to anticipate what the next stimulus condition would be.

Subject Position: The subject sat a distance of 218 cm from the face of the TV monitor. He placed his chin on a chin rest in order to properly locate and help immobilize his head. He was able to activate the electronic switch and response buttons without diverting his gaze from the screen.

CHAPTER 4

STIMULI AND RESULTS

4.1. Stimuli

In this section "stimulus" means one of the 80 non-blank stimuli presented in each experimental round. All stimuli contained either 1 or 2 half-field sinusoidal grating patches. Each patch was constant vertically, approximately 2° tall, 1° wide and ended a short distance from the center of the visual field. In order to avoid discontinuities at the borders, patches ended at zero-crossings on the sides and the tops and bottoms were tapered. Four such patches were used. Their horizontal cross sections appear as solid curves in Fig. 4.1. Frequency f_1 was $12.8 \text{ ~}/0$ and f_2 was exactly one-third of that or approximately $4.3 \text{ ~}/0$. Each patch contained more cycles than are shown. Frequency f_1 patches contained 12 full cycles, f_2 patches 4. The dashed portions of the curves show the distance from the end of each patch to the fixation point marking the center of the screen. Note that the two patches of a single frequency were in phase and that the two patches on each side were placed so that peaks added.

Stimuli were organized in groups of 5. Each group had a primary stimulus component (one of the 4 patches) and a secondary component (one of the remaining 3 patches or a blank). The contrast of the primary component was different for each stimulus in the group while that of the secondary component was held constant. Each group contributed to one of the psychometric functions shown in the curves of section 4.2. (See e.g. Fig. 4.2.) As can be seen from these curves, the 5 contrasts at which a primary patch appeared depended only upon its frequency, not upon its position (Right and left-hand presentations were averaged together in

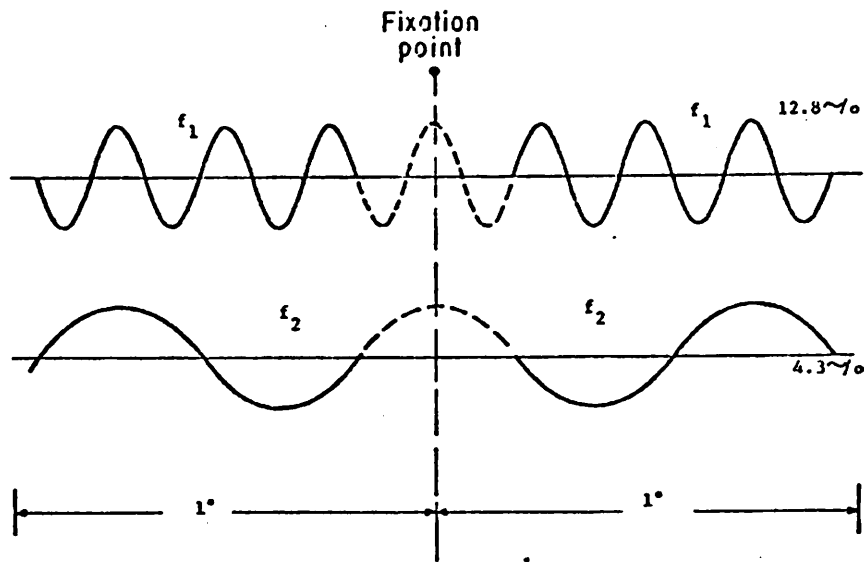


Fig. 4.1. Stimulus components. Each stimulus contained either one or two of these four unbroken patches. Note that each patch contained more cycles than are shown here - see text.

the curves -- see below.) or upon the nature of the secondary component. These 5 contrasts were chosen to match the sensitivity of the subject and were spaced 3 dB apart. Whenever a patch appeared in a secondary roll, it appeared at the second-lowest contrast which was used for it when it appeared in a primary roll. (There was one exception. See the last paragraph of section 4.2.)

Four types of secondary components were used. These are listed in Table 4.1 together with the "summation code" used for each.

Table 4.1. Stimulus Summation Code

<u>SUMMATION CODE</u>	<u>NATURE OF SECONDARY COMPONENT</u>
0	blank
1	other-frequency patch, superimposed
2	other-frequency patch, adjacent
3	same-frequency patch, adjacent

Each of the 4 patches was used as a primary patch in each of the 4 summation conditions. Thus, there were $4 \times 4 = 16$ groups and $5 \times 16 = 80$ stimuli, and each member of each group was presented exactly once per round.

Each stimulus was assigned a 4-digit label. Derivatives of these labels are used to label Figs. 4.2 through 4.7. The meaning and possible values of each digit are listed in Table 4.2.

Table 4.2. Stimulus Labels

<u>LABEL DIGIT</u>	<u>MEANING AND POSSIBLE VALUES</u>
1	Frequency of primary patch; 1 meant f_1 or 12.8 \sim /0, 2 meant f_2 or 4.3 \sim /0.
2	Summation condition; 0 through 3 as in summation code.
3	Contrast of primary patch; 1 through 5. 1 meant highest contrast, 5 lowest.
4	Position of primary patch; 1 meant left-hand side, 2 meant right.

As has been explained, all possible combinations of the above possibilities were used. This yields $2 \times 4 \times 5 \times 2 = 80$ different labels corresponding to the 80 different stimuli.

It may be helpful to give some examples. As was explained in section 2.2, the contrast of a zero mean image component is proportional to its amplitude. Here we give contrast in decibels, a unit proportional to the logarithm of component contrast (see Eq. 3.4). Subject DDS always viewed f_1 patches at one of the contrasts -37, -40, -43, -46 and -49 dB. He viewed f_2 patches at -41, -44, -47, -50 and -53 dB. Thus, whenever an $f_1(f_2)$ patch appeared as the secondary component in a stimulus, it had contrast -46 dB (-50 dB). Table 4.3 lists some examples.

One motive for choosing this set of stimuli was symmetry. The subject was instructed to center his gaze on the fixation point and to try his best to detect each stimulus. It was important that these two instructions not conflict. For example, if high contrast patches appeared more often on the right side of center, the subject might be tempted to fixate there. Several symmetries in the stimulus set prevented such biases.

<u>STIMULUS LABEL</u>	<u>CONTENTS OF LEFT SIDE</u>	<u>CONTENTS OF RIGHT SIDE</u>
1011	$f_1(-37)$	blank
1012	blank	$f_1(-37)$
1111	$f_1(-37)+f_2(-50)$	blank
1121	$f_1(-40)+f_2(-50)$	blank
1131	$f_1(-43)+f_2(-50)$	blank
1141	$f_1(-46)+f_2(-50)$	blank
1151	$f_1(-49)+f_2(-50)$	blank
1211	$f_1(-37)$	$f_2(-50)$
1311	$f_1(-37)$	$f_1(-46)$
2241	$f_2(-50)$	$f_1(-46)$
1242	$f_2(-50)$	$f_1(-46)$
2141	$f_2(-50)+f_1(-46)$	blank

Table 4.3. Sample Stimuli. For each label in the first column the second column gives the contents of the left-side of the visual field and the third column gives the contents of the right side. The presence of a patch is indicated by listing its frequency, and the contrast (subject DDS) of each patch appears in parentheses.

Frequency symmetry: Patches at frequency f_1 appeared as often as did those at f_2 .

Spatial extent symmetry: Half-blank stimuli (summation codes 0 and 1) appeared as often as did stimuli containing patches on both sides (codes 2 and 3).

Role symmetry: Each of the four patches appeared in both the primary and the secondary role. The number of times each occurred did not differ between patches.

Position symmetry: For every stimulus there existed another which was its mirror image.

The existence of position symmetry had an impact upon the use of the data. Sixty responses to each stimulus were recorded in each experimental run. However, responses to mirror-image stimuli were averaged together

yielding 120 responses per point in the curves of the next section. Labels for mirror image stimuli differed only in the last digit. Thus, for every stimulus group there existed a position symmetric group. Each such pair of groups yielded one of the psychometric functions (solid curves) of the next section.

4.2. Data

The complete experiment was performed five times. The resulting data are plotted in Figs. 4.2 through 4.6 together with some curves calculated from the data.

Data Curves

In each figure the horizontal line marked "blank rate" gives the average of 1200 responses to blank trials. The 4 numbers listed there give the false alarm rates for the 4 thresholds. Other data points represent the average of 120 subject responses and the points of a single psychometric function are connected with solid straight lines. In order to understand the labels given to these psychometric functions, let $a \in \{1,2\}$ and $b \in \{0,1,2,3\}$. Then there are two stimulus groups with primary patch at frequency f_a and summation code b . These groups are position symmetric and yield the curve labelled " ab " = $10a + b$ in the following manner. Number the five points of the curve from right to left. Then, if $c \in \{1,2,3,4,5\}$, all responses to the stimuli labelled " $abc1$ " and " $abc2$ " (" $abc1$ " = $1000a + 100b + 10c + 1$) were averaged together. In short, curve " ab " gives the subject's response when frequency a was varied in summation condition b .

Each figure contains two groups of 4 solid curves. In the group on the right the high frequency patch was always primary. Thus, curve 10 is

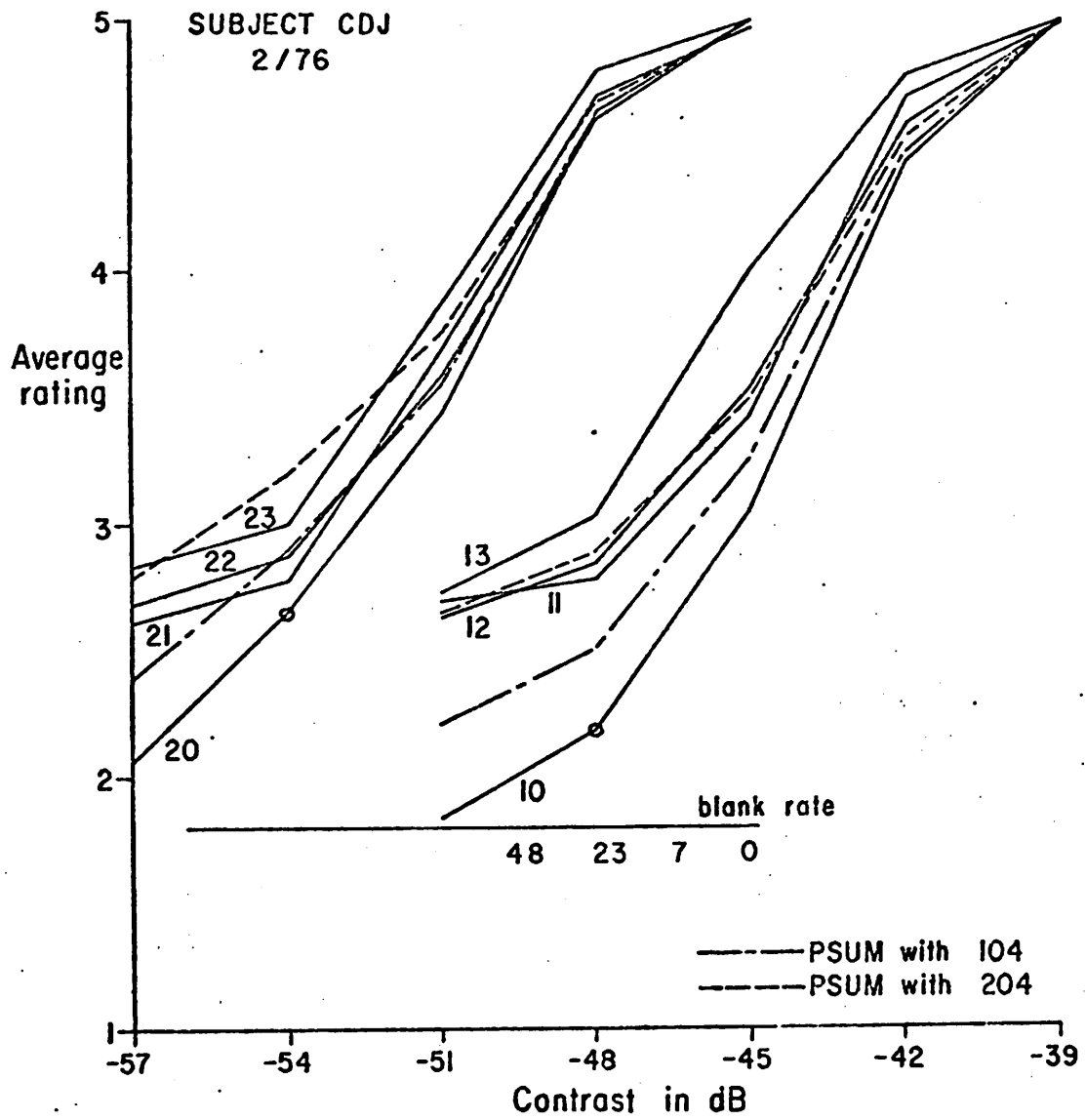


Fig. 4.2. Experimental data - see text.

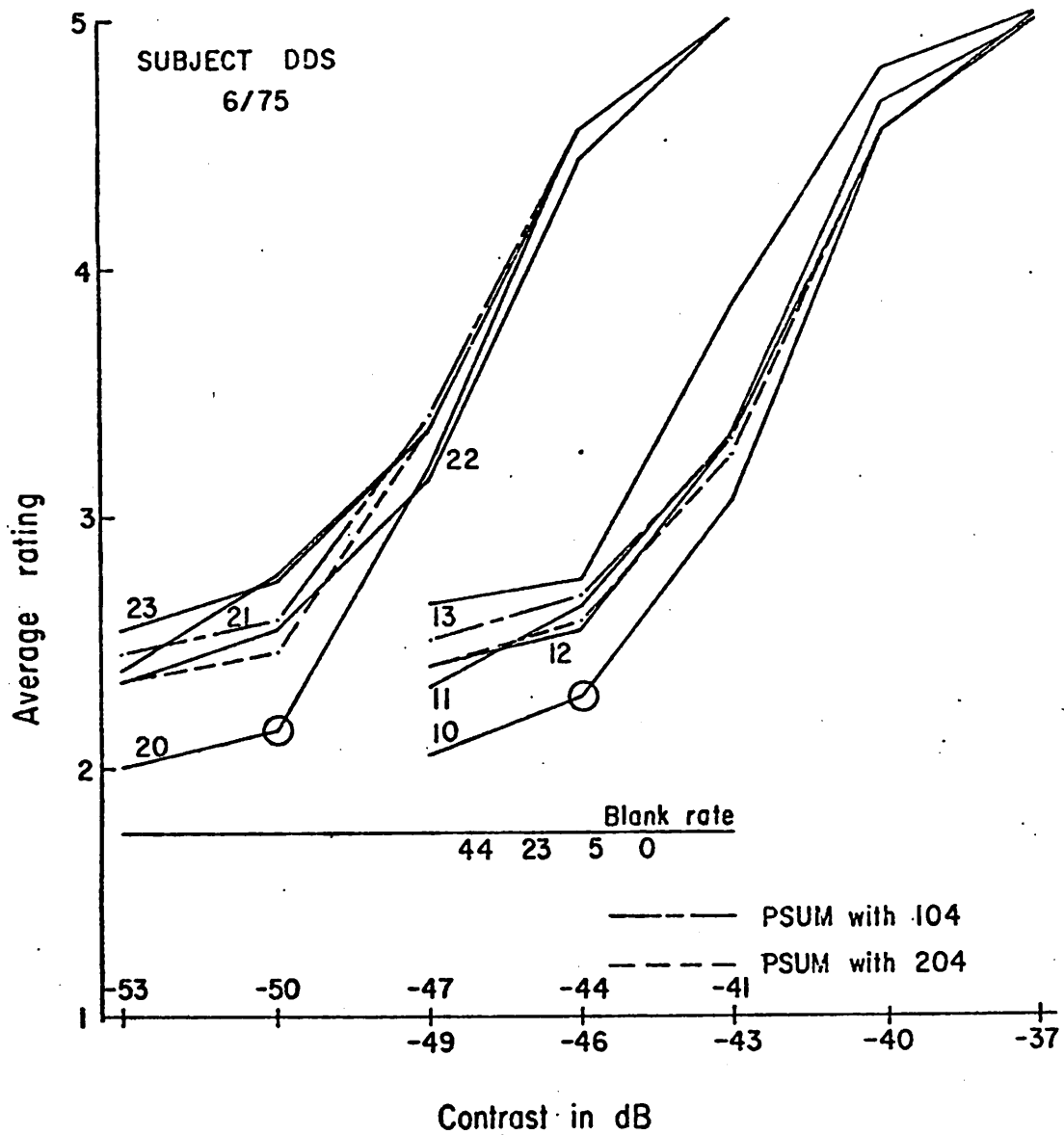


Fig. 4.3. Experimental data - see text. Groups of curves have been displaced laterally for clarity. Thus, two contrast scales are used, one for each group of curves.

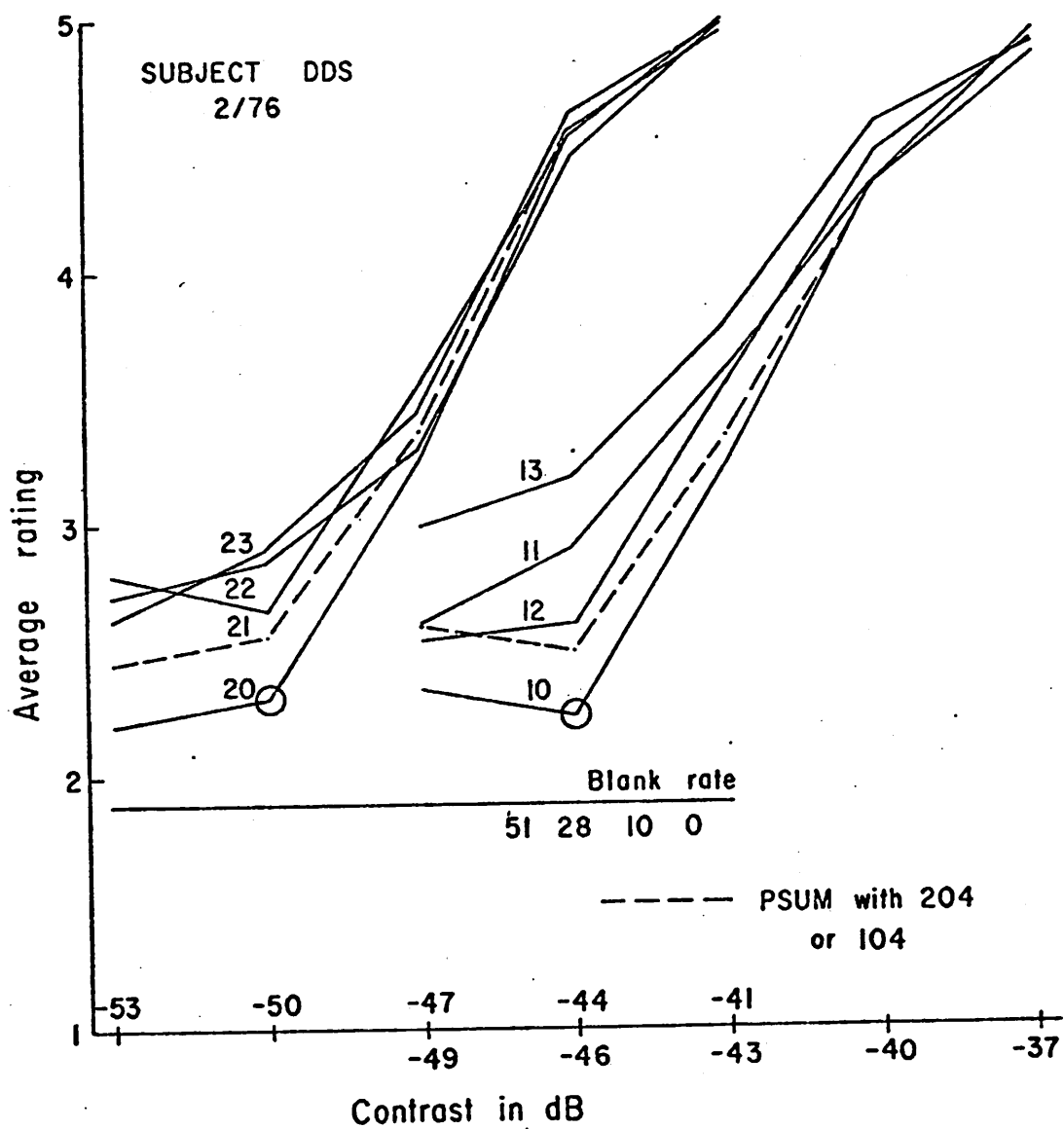


Fig. 4.4. Experimental data - see text. Groups of curves have been displaced laterately for clarity.

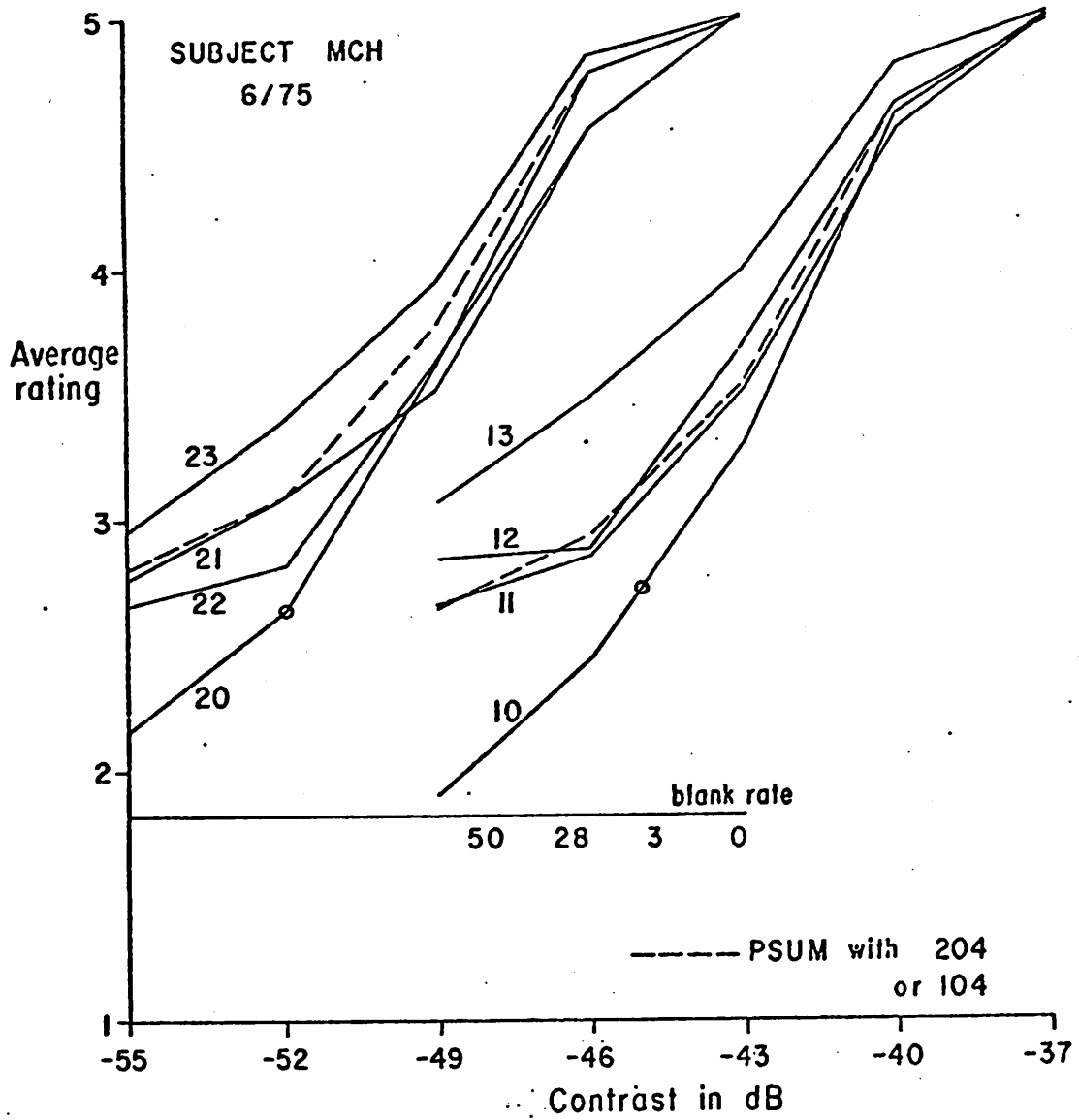


Fig. 4.5. Experimental data - see text.

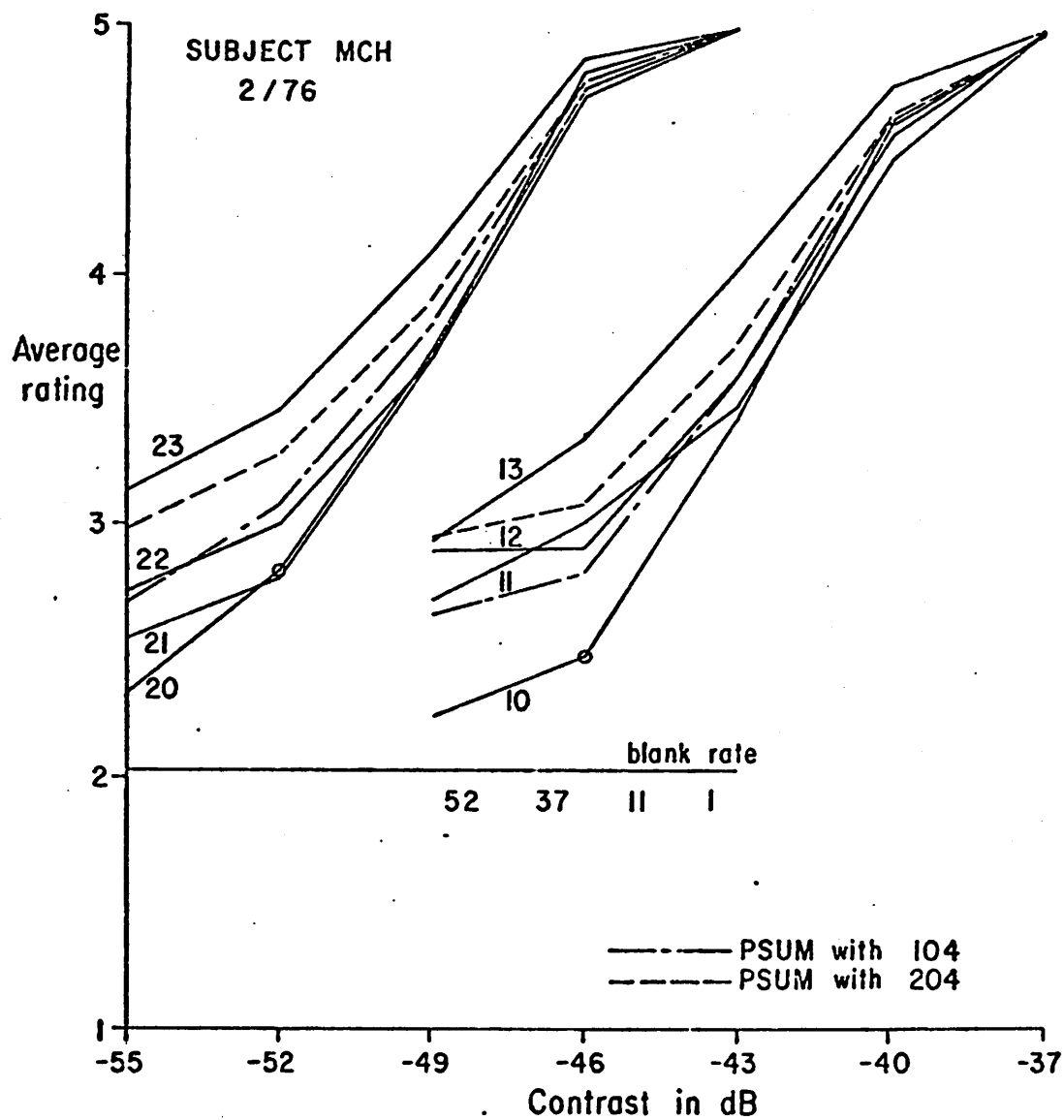


Fig. 4.6. Experimental data - see text.

for the 12.8 -/0 patch presented alone. Curve 11 is for that patch varied with level 4 (the circled point on curve 20) of a 4.3 -/0 patch superimposed. Curve 12 is for the f_2 patch adjacent, and curve 13 is for level 4 (circled point on curve 10) of the f_1 patch adjacent. The other 4 curves have a symmetrical description.

Probability Summation Curves

Section 3.2 explains the probability summation (PSUM) calculation given rating data for blanks and two stimuli. For reasons to be explained in chapter 5, this calculation was used to produce the dashed and dot-dashed curves in the figures. However, here each data point corresponds to two stimuli and thus the PSUM calculation was applied not to pairs of stimuli but to pairs of data points. The calculation remains the same, proceeding as if all of the data associated with a single data point had come from a single stimulus.

Let (p_1, p_2) represent the average response obtained via the calculation of section 3.2 from the data points p_1 and p_2 . Then in each figure, (105,204) is the PSUM of the fifth point (numbering from the right) of the 10 curve with the fourth point (it is circled.) of the 20 curve. This corresponds to the fifth point of the right-hand dashed curve. The remaining points on that curve are, in ascending order, (104,204), (103,204), (102,204) and (101, 204). In other words each point of the 10 curve has been moved upward by summing it probabilistically with the circled point on curve 20. We say that point 204 was summed with the 10 curve.

It is now easy to describe the other PSUM curves. The dashed curve in the left-hand group of curves is the summation of point 204 with the 20 curve. The dot-dashed curve in the right-hand (left-hand) group is the

summation of point 104 with curve 10 (20). Note that Figs. 4.4 and 4.5 contain no dot-dashed curves. This is due to the fact that in both cases the two circled points were at the same height. Had the dot-dashed curves been plotted, they would have overlapped the dashed curves.

Note also that in Fig. 4.5 the right-hand circle does not enclose data point number 104. These circles indicate the contrast at which the f_1 and f_2 patches appeared when in a secondary roll. Due to an error in the instructions given to the computer during this run of the experiment, this contrast for f_1 differed from that of point 104 by 1 db. As a result the subject's response was not measured at that contrast and a linear interpolation between points 104 and 103 was performed for the purposes of the PSUM calculation.

4.3. Support for the Present Use of Average Ratings

Conclusions relative to the purposes of the experiment will be discussed in chapter 5. However, it is appropriate to make one observation here because it relates to the way data were presented in the last section. A subject's sensitivity to a stimulus has been represented here by the average of his rating responses to it. Sensitivity, both classically and in the construction of the rating task, is taken to mean frequency of seeing. Classically, a subject responds "I saw it." or "I did not see it." on each trial. The more often he says "I saw it" the greater his sensitivity to the stimulus is said to be. Our rating task is constructed to yield the same measure of sensitivity but for four different thresholds at once (section 3.1). In presenting our data as we have, we assert that for our data and on every stimulus knowledge of the average response is equivalent to knowledge of the frequency of seeing for each of the four thresholds.

How might this assertion be wrong? Clearly, an average of 2.5 can result from an equal number of 2's and 3's or from an equal number of 1's, 2's, 3's and 4's (or from other combinations of responses). The threshold by threshold breakdowns of these two idealized response patterns differ greatly. In the first case the "percent see" for the first threshold is 100%. For the second it is 50%, and for the third and fourth it is 0% (see Fig. 3.1b). In the second case these figures are 75%, 50%, 25% and 0%. Thus, information present in the rating data is lost upon averaging.

Such behavior might be expected in an experiment containing stimuli such as ours. Suppose there are two stimuli which normally elicit responses at levels 1, 2 and 3. Suppose further that they are presented together in a composite stimulus and that when this stimulus is viewed the components are detected independently. Then the composite should normally elicit responses at levels 1, 2 and 3. However, more 2's and 3's will be given to the composite than to either component and the composite will yield a higher average rating. On the other hand, suppose that one of the components is presented alone but with its contrast raised to the point where it yields the same average rating as does the composite. One might expect this stimulus to elicit a significant number of responses at level 4 or 5.

Thus, we see that our assertion cannot be proven analytically. In order to support it we must test our data. The appropriate test is very straightforward. We simply examine response patterns as a function of average response. If at a given average response one type of stimulus tends to give a different response pattern than does another, then our assertion has been contradicted. If this does not happen, it has been supported.

This test takes the form of a graph in Fig. 4.7. Here the percent see at each threshold is plotted for each stimulus as a function of the average response to that stimulus. We find that for each threshold all data could be well-fit by a single smooth curve. PSUM calculations have also been plotted in the same manner. Thus, when a PSUM calculation agrees with the data on the basis of average response, it also agrees on a threshold-by-threshold basis.

Figure 4.7 gives the data for subject MCH, 2/76. All other sets of data yielded equally good support for the assertion. The curves for the four thresholds peak at 100%. Three have been displaced vertically for clarity. Because this plot contains so many points it was impossible to label them all. This matters little because the fit is so good. However, three sets of points were labelled — those for curves 10, 13 and the PSUM of data point 104 with curve 10. For example, the arrow labelled 103 marks the average rating, 3.43, for the third highest data point on the 10 curve. The topmost dot plotted directly above this arrow gives the percentage of trials on which the subject responded either 2, 3, 4 or 5 (85%). The second highest dot is for responses of 3 or greater (80%). The remaining two are for 4 or greater (55%) and 5 (22%). Only the 4 lowest points from the PSUM curve were labelled. "P2" indicates the second highest, "P3" the third highest, etc. The highest point was not labelled because it coincides exactly with point 101.

The previous discussion justifies the present use of average ratings but it does not motivate it. Why did we not employ a single-threshold response task or plot our data threshold-by-threshold? The reason is simple and basic. It is that the present approach yields more information. A rating response or, as we have just seen, an average rating gives sensitivity in terms of four thresholds rather than just one.

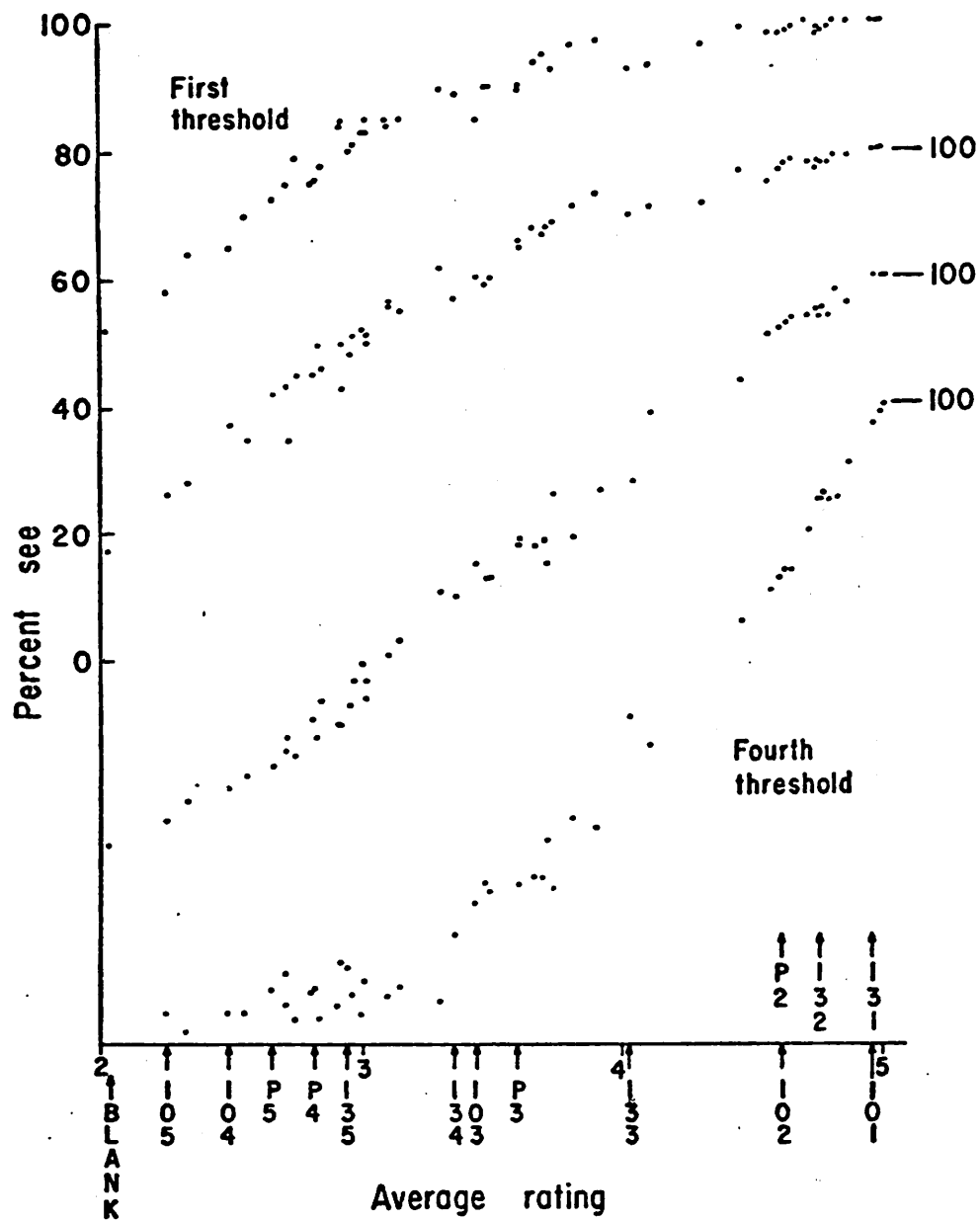


Fig. 4.7. Response patterns as a function of average response. The probability of detection is plotted for each of the four thresholds as a function of average response. The data is that from subject MCH, 2/76.

CHAPTER 5

CONCLUSIONS

In chapters 3 and 4 we explained that psychometric functions for simple (one patch) and complex (two patch) stimuli were measured. In this chapter we compare each complex psychometric function with the appropriate probability summation (PSUM) calculation. When the fit is good we conclude that component patches could have been detected by disjoint groups of independent channels. When it is poor we conclude that some single channel must have responded to portions of both patches. Next, we comment on the criterion used to make decisions about goodness of fit. Lastly, we discuss what can be learned about visual detection from these conclusions.

5.1. PSUM Comparisons -- the Test for Independence

Every data point on each complex psychometric function gives the average response to a stimulus containing two patches. The response to each patch alone was also measured. Thus (section 3.2) it was possible to calculate exactly the average response which should result if, when presented together, the two patches were detected independently. The accuracy of this PSUM prediction is assessed below for each type of complex psychometric function. The conclusion drawn in each case is the result of comparing all 5 sets of data.

Patches of Different Frequencies Superimposed

Conclusion: Independence

Curve 21 is for a low frequency patch varied in contrast with a constant amplitude high frequency patch superimposed. It should be compared with the dot-dashed curve. The fit is judged acceptable.

Curve 11 is for a high frequency patch varied with a low frequency patch superimposed. It should be compared with the dashed curve. The fit is judged acceptable.

Patches of Different Frequencies Adjacent

Conclusion: Independence

Curve 22 is for a low frequency patch varied with a high frequency patch adjacent. It should be compared with the dot-dashed curve. The fit is judged acceptable.

Curve 12 is for a high frequency patch varied adjacent to a low frequency patch. It should be compared with the dashed curve. The fit is judged acceptable.

Patches of Same Frequency Adjacent

Conclusion: The conclusion is different for each frequency.

Curve 23 is for a low frequency patch varied with a low frequency patch adjacent. It should be compared with the dashed curve. The fit is judged acceptable leading to the independence conclusion. This decision is uncertain in Figs. 4.5 and 4.6 (subject MCH). This subject consistently displayed supra-probabilistic summation. That is, the data lies above the PSUM calculation. Because the size of the difference was small and did not occur for the other two subjects, we did not consider it conclusive.

Curve 13 is for a high frequency patch varied with a high frequency patch adjacent. It should be compared with the dot-dashed curve. The fit was judged unacceptable. For all subjects and at all but the highest contrasts the data lies above the calculation. In most cases the difference is quite large. We conclude that there was facilitory interaction between the patches. Thus, they could not have been detected independently.

There must have been at least one active channel which overlapped portions of both patches.

5.2. Criterion for Judgements on Goodness of Fit

Throughout this discussion we have acknowledged that visual detection is a noisy process. Our scheme for data collection, plotting, and evaluation is a response to this fact. However, the nature (i.e. additive, multiplicative, etc.) and distribution of system noise has not been modelled to our satisfaction. For that reason we offer no parametric fits to our psychometric functions or statistical tests of our decisions regarding goodness of fit. Instead, we rely upon our experience with data of this type. In this section we point out ways in which the reader may estimate the noise in the data for himself.

In chapter 4 stimuli were described in groups of 5. This suited the purposes of the experiment because each group was associated with one of the psychometric functions. However, in some instances this grouping was very artificial. For example, responses to stimuli 2241 and 1242 were collected, recorded, averaged and plotted independently, as if they had been any other pair of stimuli. Yet they were physically identical. (Both of these stimuli had level 4 of the low frequency patch on the left-side with level 4 of the high frequency patch on the right -- see Table 4.3.) The same was true of stimuli 2242 and 1241. Thus, points 224 and 124 on each data plot represent two estimates of system response to the same input. The same is true of points 214 and 114 (Table 4.3).

If there were no noise in the data these pairs of points would always appear at the same height (average rating) in our plots. Thus, by comparing these special pairs of points on each of the data plots, one may

make an estimate of the typical noise in a data point. For example, in Fig. 4.3 subject DDS gave identical responses (2.55) at points 224 and 124. Eight months later (Fig. 4.4) the same subject's responses at these points differed by $.26 = 2.85 - 2.59$. Therefore, in comparing a psychometric function with a PSUM calculation, we must not reject the possibility of a fit on the basis of a .25 discrepancy at one point. On the other hand, if such a discrepancy occurs at 3 or 4 points and always in the same direction, we must question the fit. Noise samples are not always large or of the same sign.

The data yields other noise estimates. Each psychometric function should be a monotonically increasing function of contrast. When this does not occur it is because of noise in the data. Also, we are confident that none of our patches are able to inhibit the detection of another. Thus, complex psychometric functions should always lie on or above corresponding simple ones. When this does not occur it is attributed to noise. Lastly, standard errors in data points ranged from 0 at an average rating of 5.0 to approximately 0.11 for average ratings between 2.0 and 3.5 (all subjects).

All of these observations indicate what kind of differences can be expected between points which would be identical in the absence of noise. Some differences will be large (.25 and larger) and some will be small, some positive and some negative. Building on this knowledge, we accepted a fit between a psychometric function and a PSUM curve unless there was both pattern and size to pointwise differences. Certainly, there is imprecision in this criterion and uncertainty in our conclusions. However, there is one comparison for which our criterion seems fully adequate. The fit of curve 13 to its PSUM curve is bad. This conclusion holds in every

one of the 5 experimental runs which were performed. These runs involved 3 different subjects, two performing two runs 8 months apart.

5.3. Conclusions Regarding the Modelling of Visual Detection

The present data supports two types of conclusions. The first is that a channel type model for detection remains viable. The second is that the detection of a moderately high frequency sinusoidal grating involves a single channel which is both frequency selective and spatially broad.

Support for the Channel Model

The concept of a channel model is supported whenever a complex stimulus is detected as if its components were processed independently. This result was expected when components at different frequencies were superimposed (curves 11 and 12) because this test is essentially a repeat of the work of Sachs, Nachmias and Robson [6]. However, in the present case the test was somewhat more stringent because our probability summation curves were not adjusted in any manner for fit with the complex psychometric functions. We conclude as they did that the detection of sinusoidal gratings can be modelled with channels and that these channels are frequency selective.

The stimulus components used to develop curves 12 and 22 were again at different frequencies, but here they were also spatially disjoint. It was expected that, if the existence of frequency selective channels was confirmed for spatially coincident stimuli, it should also occur for spatially disjoint stimuli. This proved true and constitutes a second indication that detection can be modelled with channels.

Curve 23 is for low frequency patches placed adjacent to each other. Once more the data fits a channel model. However, in this case the

channels are spatially selective. This result is wholly consistent with the work of Kulikowski and King-Smith [11]. In fact, their data deals most extensively with the detection of a 4 \sim /0 sinusoidal grating. Since our lower frequency, 4.3 \sim /0, was very close to this, this portion of the experiment could be viewed as a repeat of part of their test.

A Single Channel

The primary purpose of this experiment was to determine whether spatially disjoint portions of a single sinusoidal grating are detected by independent channels. We have already observed that this appears to be true at frequencies around 4 \sim /0. In this subsection we discuss a different result at 12.8 \sim /0.

We have concluded that when two 12.8 \sim /0 patches were presented adjacent, at least one active channel overlapped portions of both patches. Of course there may be one channel, one like those of the Frequency Channel Model, which overlaps all of both patches, but this cannot be proven with the present data. What the data does yield is an estimate of the minimum width of the two-patch channel(s). At this frequency the patches were separated by 1.5 cycles. If we assume that for a channel to respond significantly to a patch it must overlap that patch by at least 1 cycle, we must conclude that the channel in question is at least 3.5 cycles wide. In fact, it is difficult to imagine that a channel which is that narrow can explain the data. The discrepancy between the 13 curve and its PSUM curve was large. A channel which is 3.5 cycles wide must be centered on the blank area between patches if its tails are to overlap both patches. Thus, if this is the maximum width of channels at this frequency, there was only one channel responsible for the supra-probabilistic result. It

is unlikely that a single channel, stimulated only on the tails, would respond strongly enough to cause the discrepancy which was measured. For example, consider Kulikowski and King-Smith's assertion that center-surround mechanisms (line detectors, Fig. 2.3) are responsible for the detection of 4 π /0 sinusoids. The tails of one of those mechanisms certainly overlapped both patches of each 23 stimulus but without measurable result. Thus, we suggest that at frequency 12.8 π /0 there is at least one channel which is 5 or more cycles wide. A channel of this width, centered between the adjacent patches, would be rather fully stimulated and could respond strongly. Further, if such channels exist there might be several, each with a different centerpoint, which could touch both patches.

We have given a lower bound for the spatial width of a single channel. In so doing we have associated that channel with the frequency 12.8 π /0 and stated its width in cycles. This is appropriate because the channel is frequency selective -- it (apparently) did not respond to both patches of 12 or 11 stimuli. However, it is not essential that this result be described in these terms. What has been demonstrated is the existence of a single channel which is both pattern selective and broad in comparison with pattern features (grating bars).

Frequency Dependence of the Supra-probabilistic Result

It is curious that we found same-channel processing of spatially separate stimulus components at one frequency (12.8 π /0) but not at the other (4.3 π /0). Robson [10] measured the detectability of sinusoidal gratings as a function of their width. When he plotted sensitivity as a function of the number of cycles in the grating, he found that the shape of his curves did not vary when the frequency of the grating changed. Robson [13]

also measured the detectability of a vertical sinusoidal grating as a function of its position within the visual field. He found that sensitivity decreased exponentially with lateral displacement from the center of the visual field. When this displacement was measured in number of cycles (at the frequency of the grating being displayed and detected), the rate of decay was constant with respect to grating frequency. Both of these findings indicate that the detection mechanisms at different frequencies are similar. That is, that they are spatially scaled (and amplitude scaled) versions of each other. Indeed, since a wide grating differs from a narrow one in that non-overlapping bars have been added, the first finding indicates similarity in the way spatially disjoint components are summed at different frequencies. To our knowledge, no previous evidence has challenged this similarity assumption, yet the present experiment certainly does. The data at 4.3 \sim /0 can be modelled with center-surround mechanisms and that at 12.8 \sim /0 cannot.

The Frequency Channel Model

What do the present findings indicate about the Frequency Channel Model? The FCM is comprised of independent channels which are both frequency selective and spatially broad. The present experiment has reconfirmed evidence for the existence of frequency selective channels but at one frequency, 4.3 \sim /0, it has supported Kulikowski and King-Smith's proposition that channels are also spatially selective. However, at 12.8 \sim /0 we find some spatial breadth. The data does not demonstrate single channel width comparable to the spatial summation measured by Robson [10], but on the other hand, it cannot be explained with center-surround mechanisms. Thus, it appears that the FCM is incomplete but not

altogether inaccurate. It needs to be expanded but should not yet be discarded. In particular, high frequency image components (image detail) are very important for image fidelity, and it is for the detection of these that the FCM remains the most plausible model.

APPENDIX

OTHER EXPERIMENTS

Several other experiments were performed in the course of this research. They were not included in the previous chapters because we felt that they provided no clear, new information about visual detection. We present them here in summary form because they do give background information on both the properties of visual detection and the rationale used to study those properties in this research.

Some of these experiments, those in sections A.6 through A.8, do have a direct bearing on the interpretation of the data of chapter 4. Perhaps the main result in chapter 4 is that curve 13 lies above the appropriate dot-dashed curve in Figs. 4.2 through 4.6. As explained in chapter 5, this supra-probabilistic result means that some single channel involved in the detection of a 12.8 \sim /0 sinusoidal grating spans more than 3 cycles of that grating. The experiments of sections A.6 through A.8 provide a very similar test for the same supra-probabilistic result. However, in these experiments the finding was, at best, equivocal.

Despite this fact, we retain good confidence in the conclusions of chapter 5. This confidence is based in part upon the repeatability of the results of the earlier experiment. (See the last paragraph of section A.8.) It is also based upon our feeling that the experiment of chapter 4 is a superior experiment. The experiments of sections A.6 through A.8 permit comparison of a subject's response to two adjacent 12.8 \sim /0 patches with the calculated probabilistic summation behavior. The experiment of chapter 4 permits this comparison and more. In that experiment the subjects also responded to 12.8 \sim /0 patches summed with

4.3 ~/0 patches. As has been explained (chapter 2), the results of other investigations indicate that the summation of such patches should be probabilistic. The data of chapter 4 support that belief, but they also provide a standard of comparison for same-frequency summation. Curve 13 (Figs. 4.2 through 4.6) not only lies above the dot-dashed curve, it also lies above curves 11 and 12. This means that a 12.8 ~/0 patch sums more strongly with another at the same frequency than it does with a 4.3 ~/0 patch. This finding, even in the absence of a direct check for probabilistic summation, is sufficient for the conclusion of chapter 5. Nonetheless, the reader may wish to take the experiments of sections A.6 through A.8 into account when evaluating the results in chapter 4.

The experiments of this appendix are organized in chronological order and each is given a name. These names are meant for reference only and no attempt is made to explain their meaning. All aspects of experimental procedure which are not stated were identical to those discussed in chapters 3 and 4. For example, only non-blank stimuli are described. In all cases approximately 20 percent of the trials in each experimental round were blanks. This percentage was not strictly adhered to in the experiments of sections A.1 through A.4. These experiments were performed without computer control. That is, all stimulus display equipment was as in Fig. 3.2 but all computer functions were performed manually.

The conventions of chapter 4 are followed in plotting the data. In particular, data points are connected with solid, straight lines and probability summation calculations are shown dashed. The experiments of sections A.5 through A.8 were performed under computer control. The four numbers appearing under the "blank rate" line in each of the graphs of

these sections give the false alarm rates for the four thresholds used in the rating task. Some graphs contain circled data points. As in chapter 4, this always indicates the contrast at which the corresponding patch appeared when acting as the secondary component in a two-patch stimulus. Each circled point contributed to a probability summation calculation in the manner of section 4.2.

Finally, all experiments employed patches of sinusoidal gratings as stimuli. Many of these patches were identical to those of Fig. 4.1. The others were similar in that they were oriented vertically, ended at zero crossings at the sides, were approximately one degree tall, and were tapered at the top and bottom.

A.1. Patches (9-10/73)

<u>STIMULUS NUMBER</u>	<u>STIMULUS DESCRIPTION</u>
1	One 2.5 cycle wide patch of a 12.8 \sim /0 sinusoidal grating. The patch had a peak at its center and was itself centered at the center of the visual field.
2	Three patches like that of stimulus 1. One was in the center. The other two were to the left and right of center with a 4.5 cycle wide blank space between each side patch and the center patch. This spacing meant that all patches were in phase.
3	Same as 2 but with 4.25 cycle spacing, making each side patch 90 degrees out of phase with the center patch.
4	Same as 2 but with 4.0 cycle spacing making each side patch 180 degrees out of phase with the center patch.

Results: The data are plotted in Figs. A.1 and A.2. Each data point represents 35 responses. Stimuli 2, 3 and 4 were detected almost as easily as was stimulus 1. Thus, the effect of the side patches was very slight. However, subject DDS showed a slight preference for stimulus 3

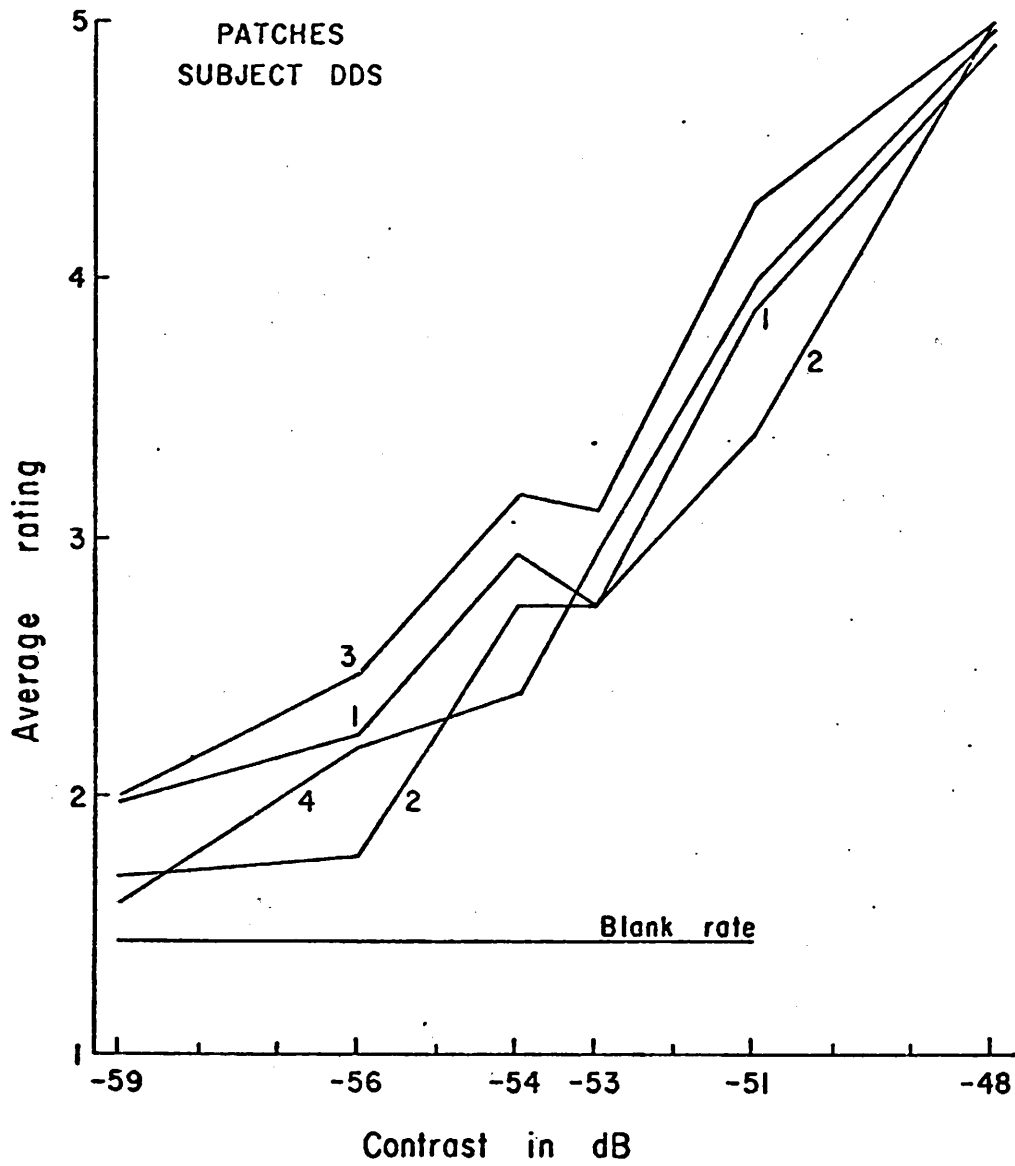


Fig. A.1. Data - "Patches" experiment.

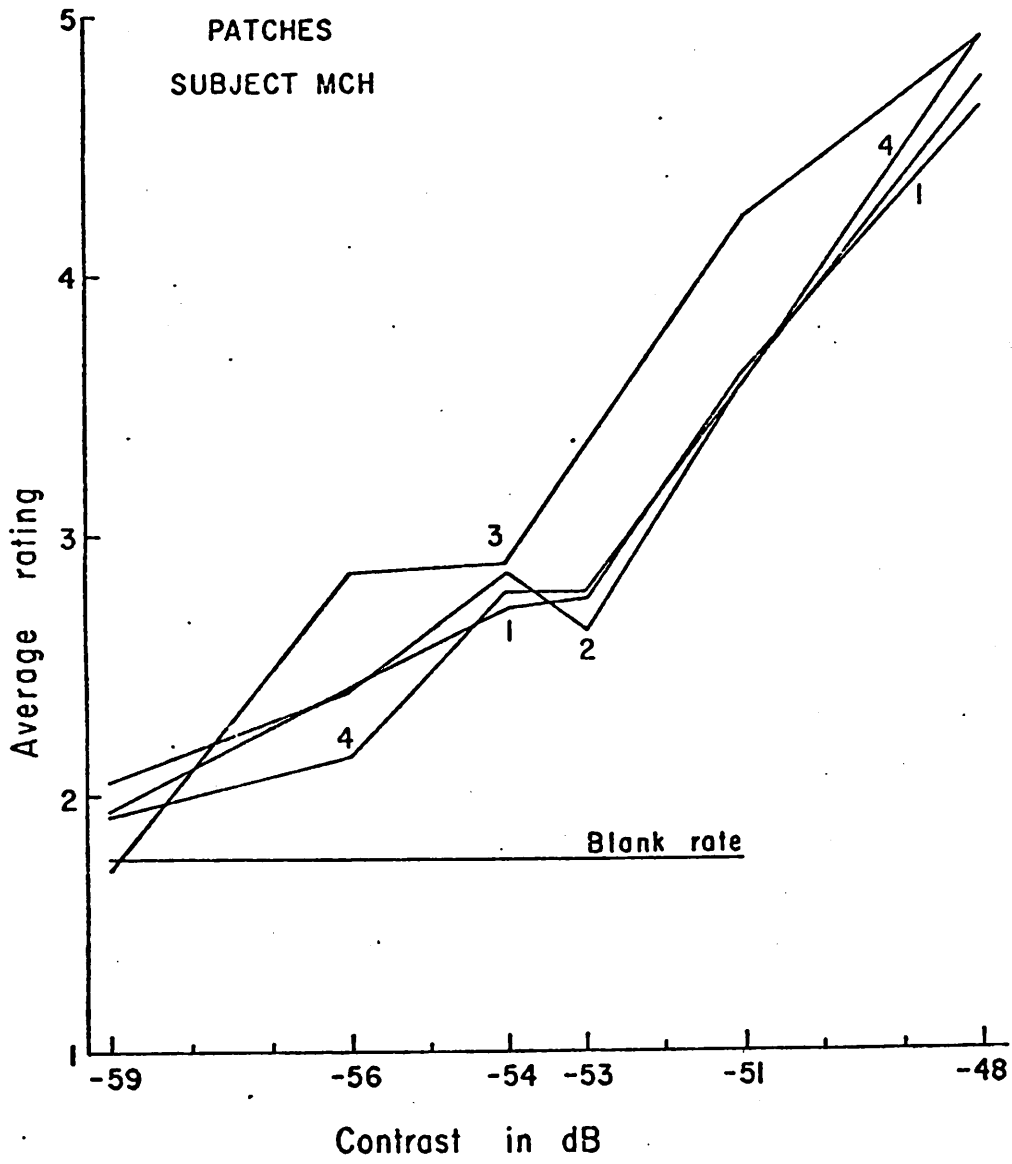


Fig. A.2. Data - "Patches" experiment.

(90 degree phase difference between adjacent patches). Subject MCH showed strong preference for stimulus 3. Psychometric functions for the other three stimuli were tightly grouped (subject MCH).

Conclusions: This phasing preference seemed questionable, especially in view of the broad spacing between patches. We decided to do "Patches II."

A.2. Patches II (1/74)

<u>STIMULUS NUMBER</u>	<u>STIMULUS DESCRIPTION</u>
1	Same as 1 of Patches.
2	Same as 2 of Patches but with 2.5 cycle inter-patch spacing. (Adjacent patches were in phase.)
3	Same as 2 but with 2.25 cycle spacing. (90 degrees out of phase).
4	Same as 2 but with 2.0 cycle spacing. (180 degrees out of phase)
5	Same as 2 but with 1.75 cycle spacing. (270 degrees out of phase).
6	Unbroken grating (sinusoid at 12.8 ~/0) 12.5 cycles wide.

Results: The data are plotted in Figs. A.3 and A.4. Each data point represents 42 responses. Little could be determined from the data of Fig. A.4. However, subject DDS gave very similar responses to stimuli 2 through 4.

Conclusions: The relative phasing of adjacent patches did not affect their detectability. Thus, it appears that spatially disjoint portions of a sinusoidal grating are detected incoherently. However, spatial coherence has not been strictly ruled out. The patches of stimuli 3, 4 and

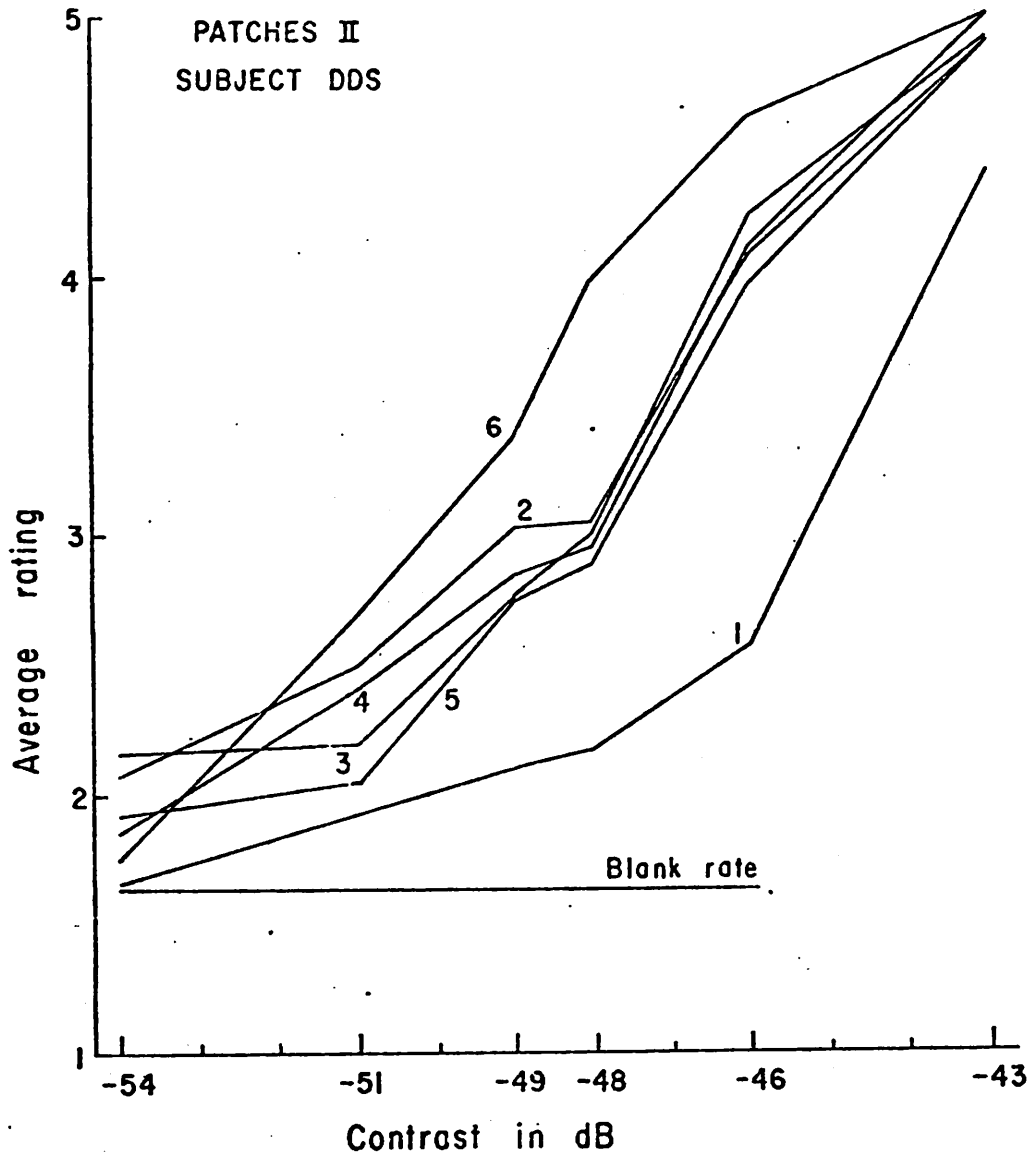


Fig. A.3. Data - "Patches II" experiment.

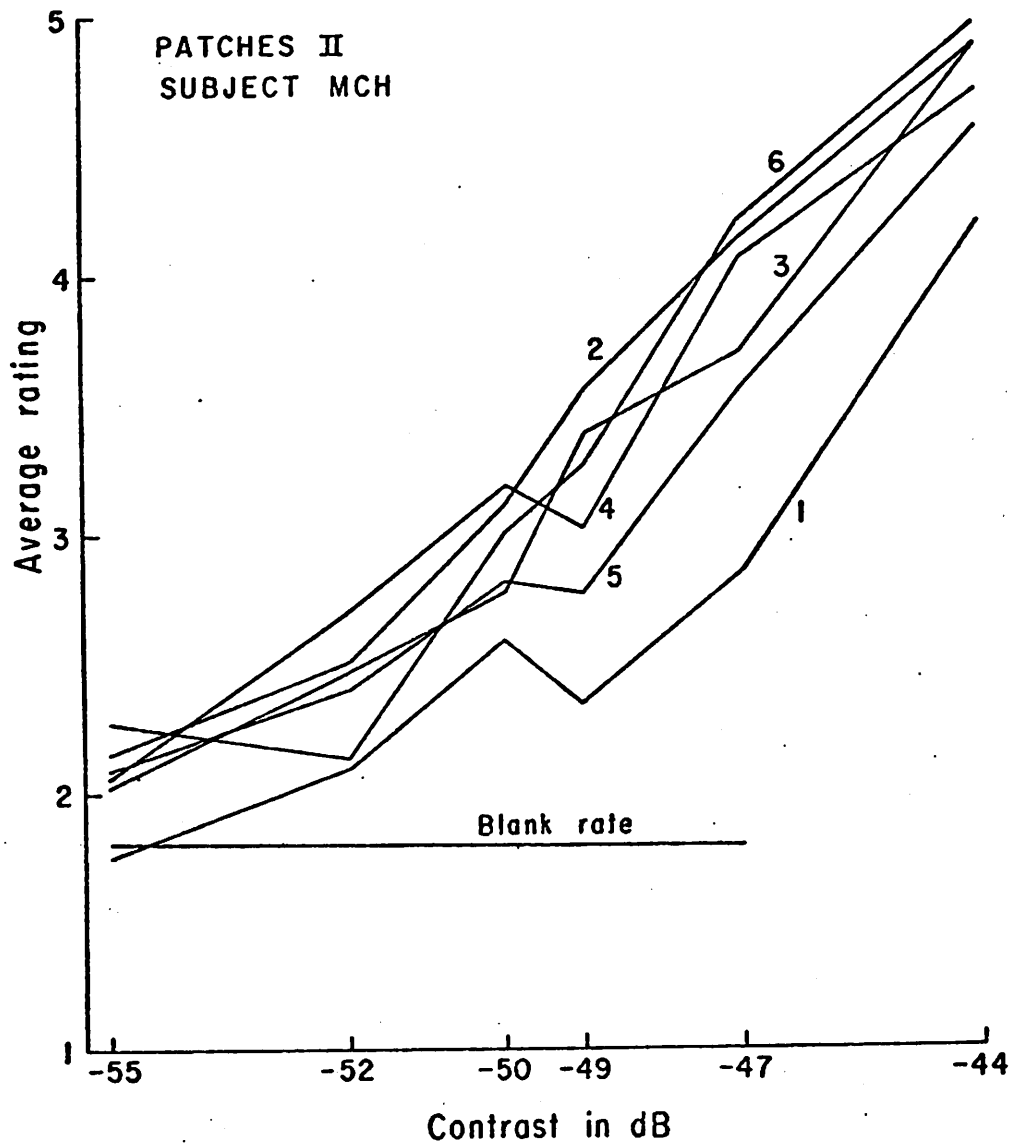


Fig. A.4. Data - "Patches II" experiment.

5 were incoherent at frequency 12.8 \pm 0 but would register well with gratings at slightly higher or lower frequencies. Thus, detection of these stimuli might have been accomplished coherently by mechanisms "tuned" to frequencies above or below 12.8 \pm 0. It was decided that an experiment should be performed which might show whether or not the same mechanism was responsible for the detection of each of stimuli 2 through 5.

A.3. Channel Shift - Phase I (7/74)

<u>STIMULUS NUMBER</u>	<u>STIMULUS DESCRIPTION</u>
1	Same as the first stimulus in both "Patches" experiments but here the patch was only 1.5 cycles wide.
2	Contained the central 1.5 cycle patch of 1 together with two side patches. Side patches were 3 cycles wide and spaced 0.5 cycles from the center patch. This spacing caused adjacent patches to be in phase.
3	Same as 2 but with 1 \sim spacing. Thus, adjacent patches were 180° degrees out of phase.
4	Same as 2 but with 1.5 \sim spacing. (In phase).
5	Same as 2 but with 2 \sim spacing. (180° out of phase)

Results: The data, 44 responses per point, are plotted in Figs. A.5 and A.6. For both subjects stimulus 3 was clearly the most detectable.

Conclusions: This result is different from that of Patches II -- one spacing was preferred over the others. It was decided that we should attempt to repeat this finding.

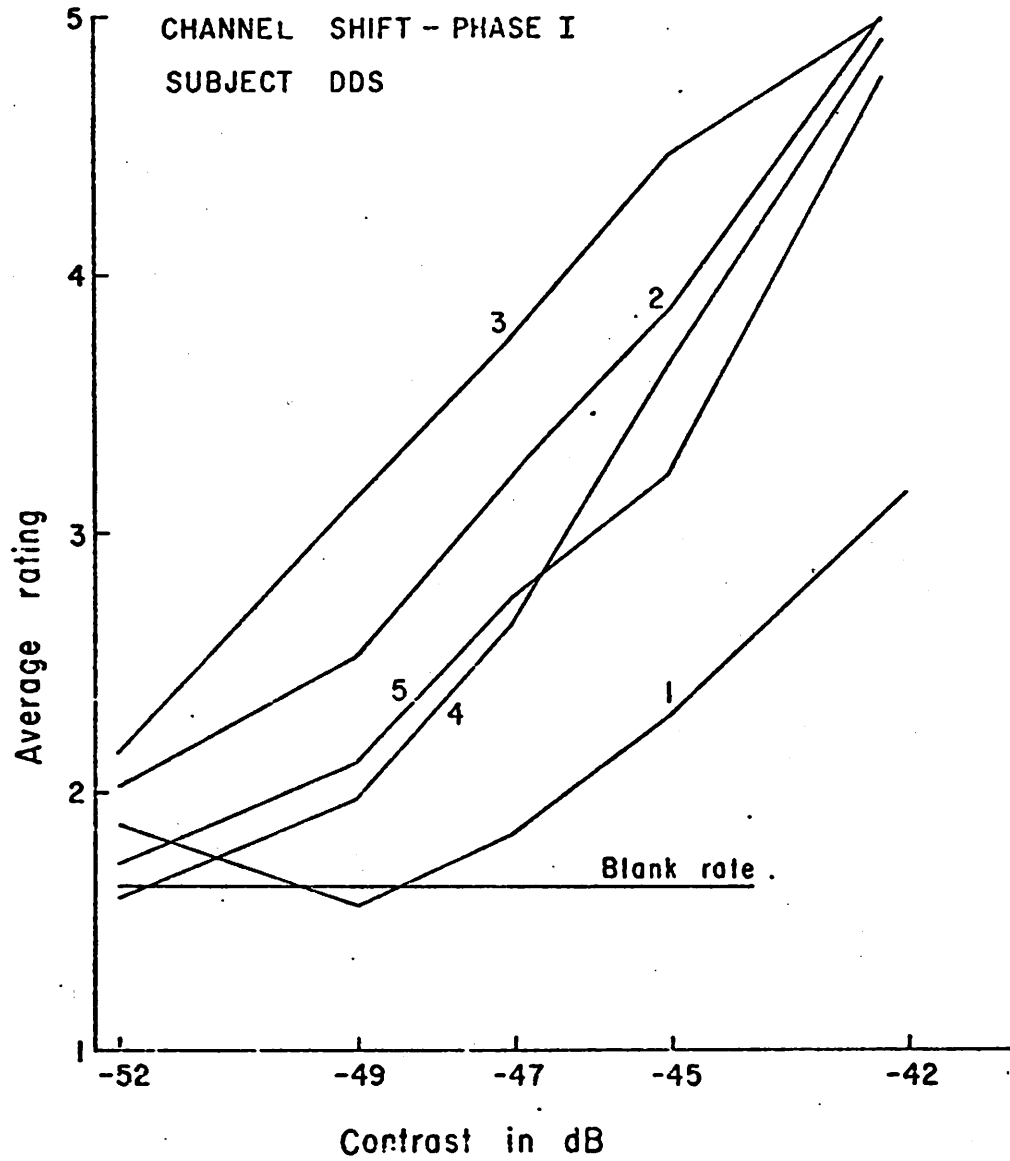


Fig. A.5. Data - "Channel Shift - Phase I" experiment.

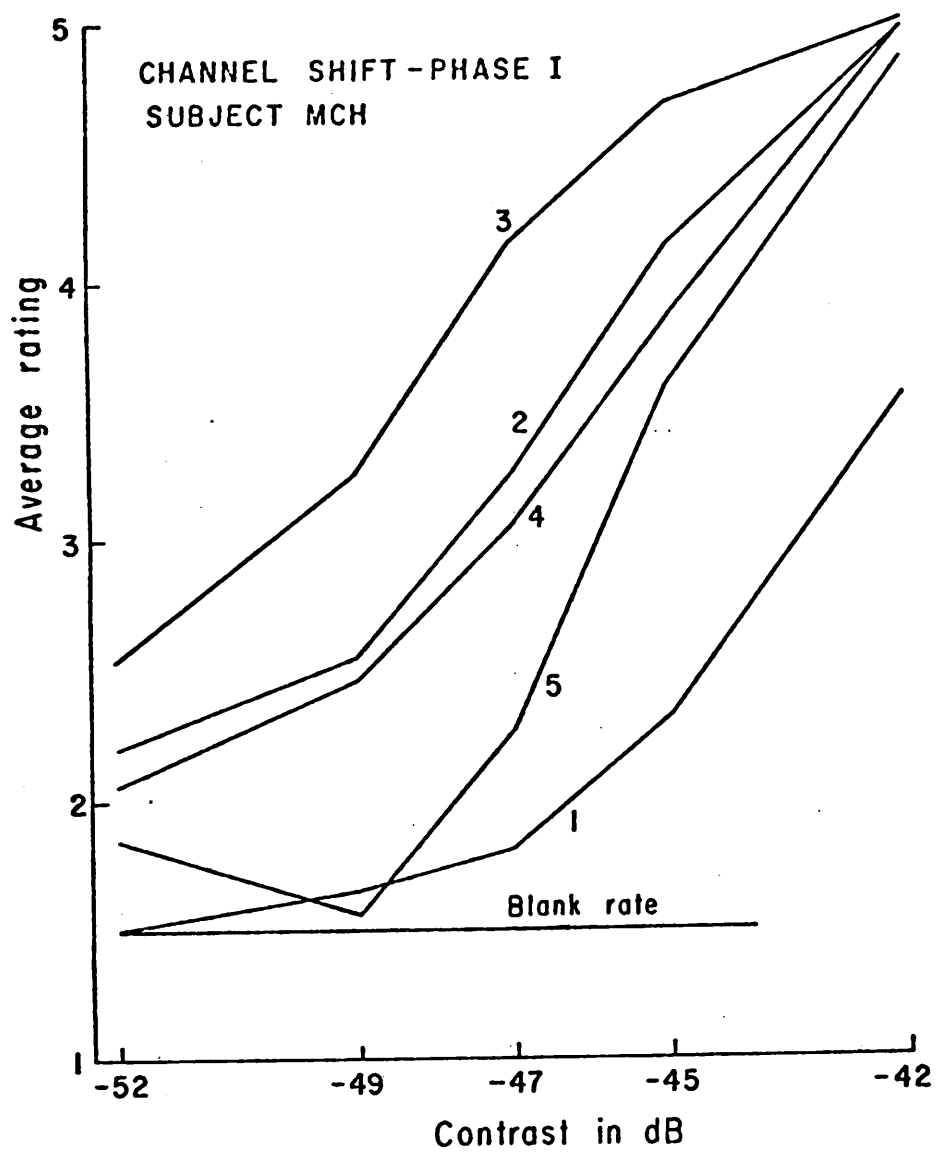


Fig. A.6. Data - "Channel Shift - Phase I" experiment.

A.4. Channel Shift - Phase II (8/74)

<u>STIMULUS NUMBER</u>	<u>STIMULUS DESCRIPTION</u>
1	Unbroken sinusoidal grating, 9.5 cycles wide, frequency 12.8 \sim /0.
2	Same as 2 of Phase I.
3	Same as 3 of Phase I.

Results: The data, 24 responses per point, are plotted in Figs. A.7 and A.8. Subject DDS detected stimuli 2 and 3 equally well. Subject MCH detected stimulus 2 more easily than stimulus 3.

Conclusions: These results are in disagreement with those of Phase I. In Phase I stimulus 3 was found to be more detectable than stimulus 2. Thus, on the basis of experiments A.1 through A.4 we concluded that the relative phasing of adjacent patches had no effect upon detectability. However, our confidence in this result was weakened by the apparent instability of the result. The question of a channel shift, the possibility that when inter-patch spacing is changed visual mechanisms tuned to different frequencies come into play, remained unanswered.

A.5. "P" (5/75)

This is the first experiment performed under computer control. The stimuli contain the patches of Fig. 4.1. In the table below the presence of a patch is indicated by listing its frequency, $f_1 = 12.8 \sim$ /0, $f_2 = 4.3 \sim$ /0. When a stimulus contained two patches, stimuli 3 and 6, both patches always appeared at equal contrast.

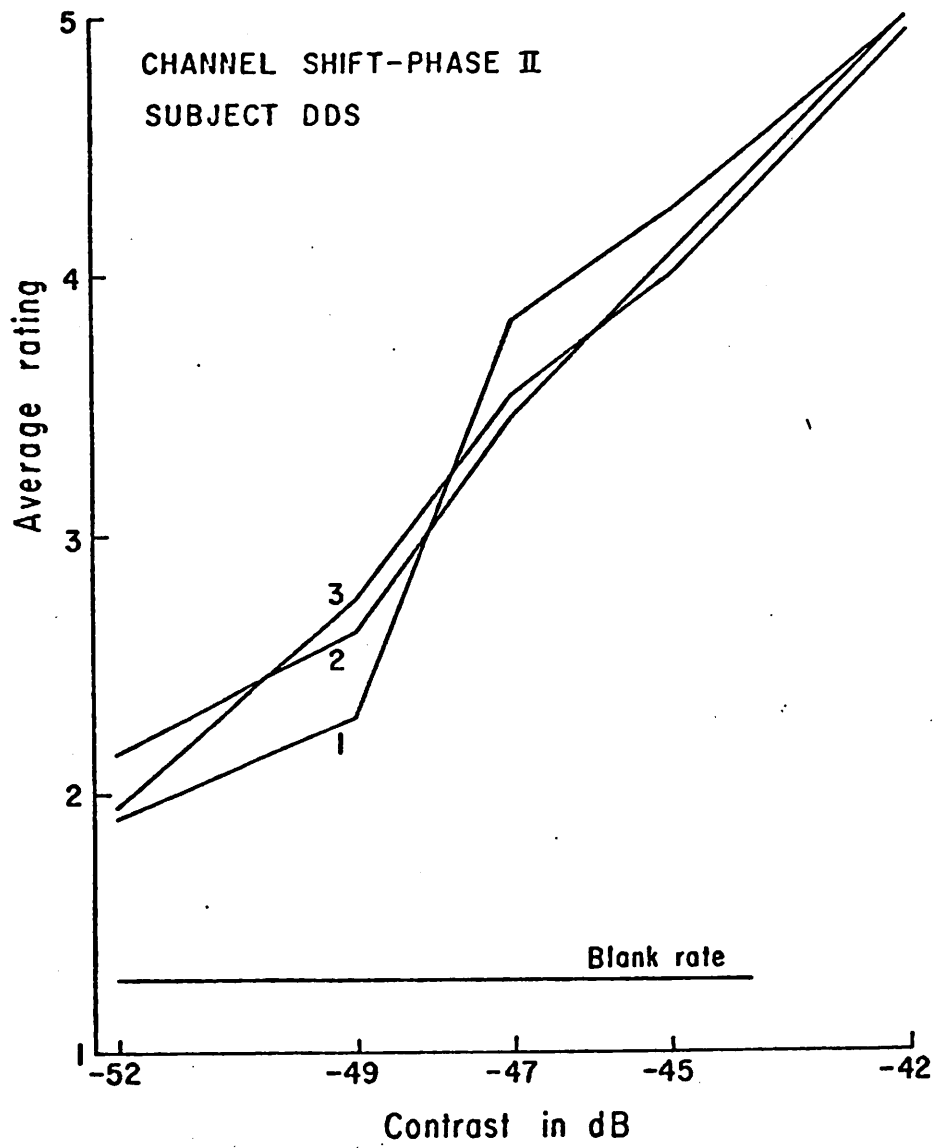


Fig. A.7. Data - "Channel Shift - Phase II" experiment.

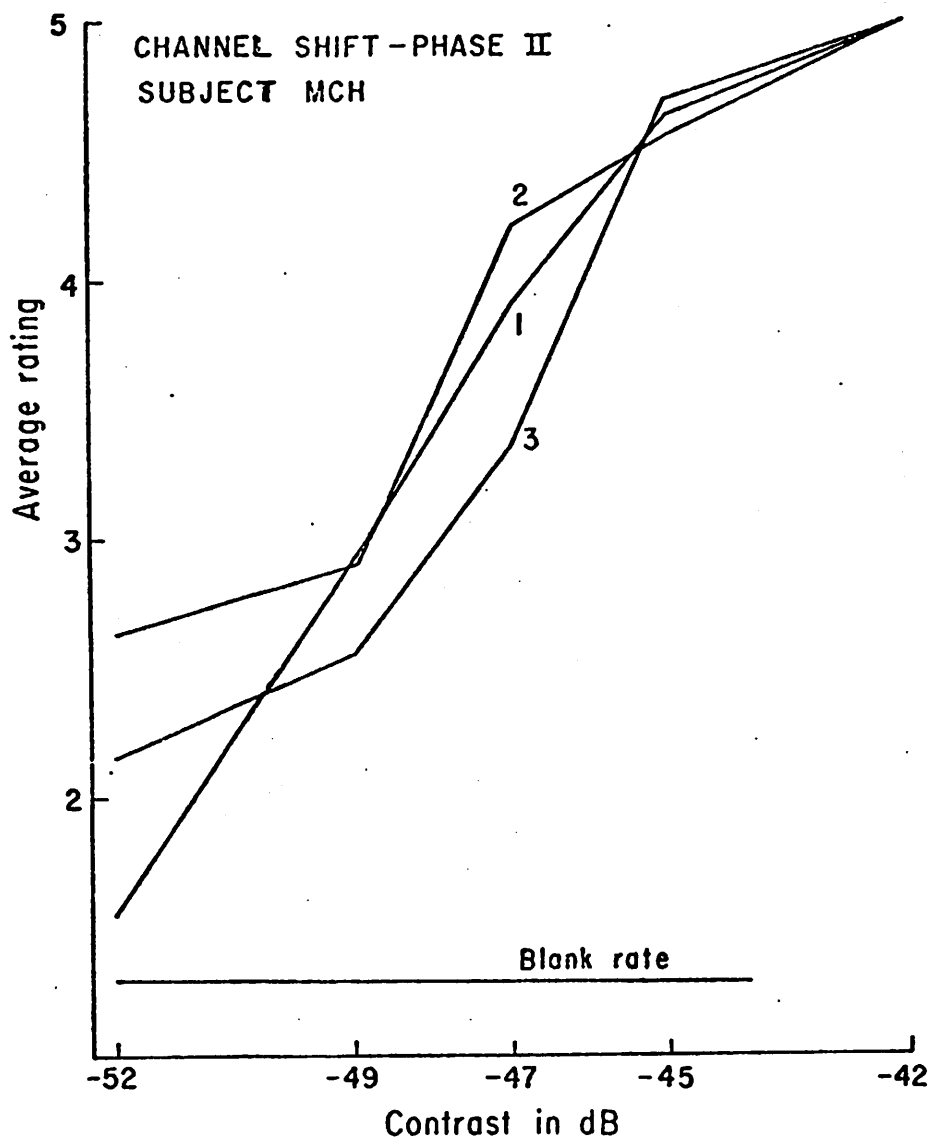


Fig. A.8. Data - "Channel Shift - Phase II" experiment.

<u>STIMULUS NUMBER</u>	<u>CONTENTS OF LEFT SIDE OF VISUAL FIELD</u>	<u>CONTENTS OF RIGHT SIDE OF VISUAL FIELD</u>
1	f_1	blank
2	blank	f_1
3	f_1	f_1
4	f_2	blank
5	blank	f_2
6	f_2	f_2

Results: The responses to stimuli 1 and 2 (4 and 5) were averaged together yielding the curve marked 12 (45) on Figs. A.9 and A.10. Thus, curves 3 and 6 in each of those figures represent 48 responses per data point whereas curves 12 and 45 represent 96 responses per data point. The dashed curve on the right side of each graph represents the probability summation of the responses to stimuli 1 and 2. Thus, if when stimulus 3 was presented the two patches were detected independently, curve 3 should coincide with this dashed curve. The dashed curve on the left has a similar meaning.

Conclusions: The primary purpose of this experiment was to acquaint the subjects with the computer-controlled experimental procedure and with the patches used in the experiment of the previous chapters. The stimulus set was not symmetric in the sense that full-field stimuli occurred only half as frequently as did half-field stimuli. For these reasons we draw no conclusions from this data.

A.6. Coherence (9/75)

Two types of patches were used to construct the stimuli of this experiment. Each type could appear on either side of the visual field.

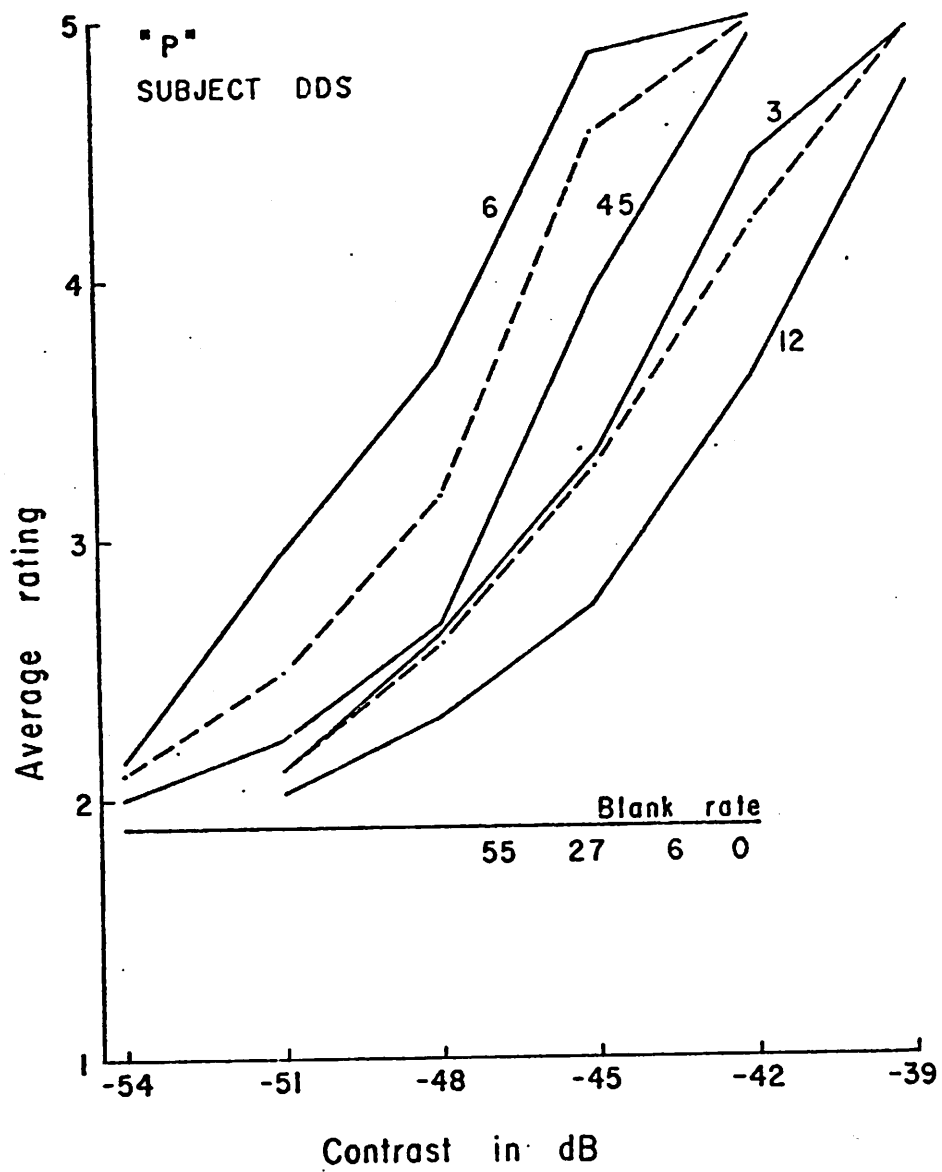


Fig. A.9. Data - "P" experiment.

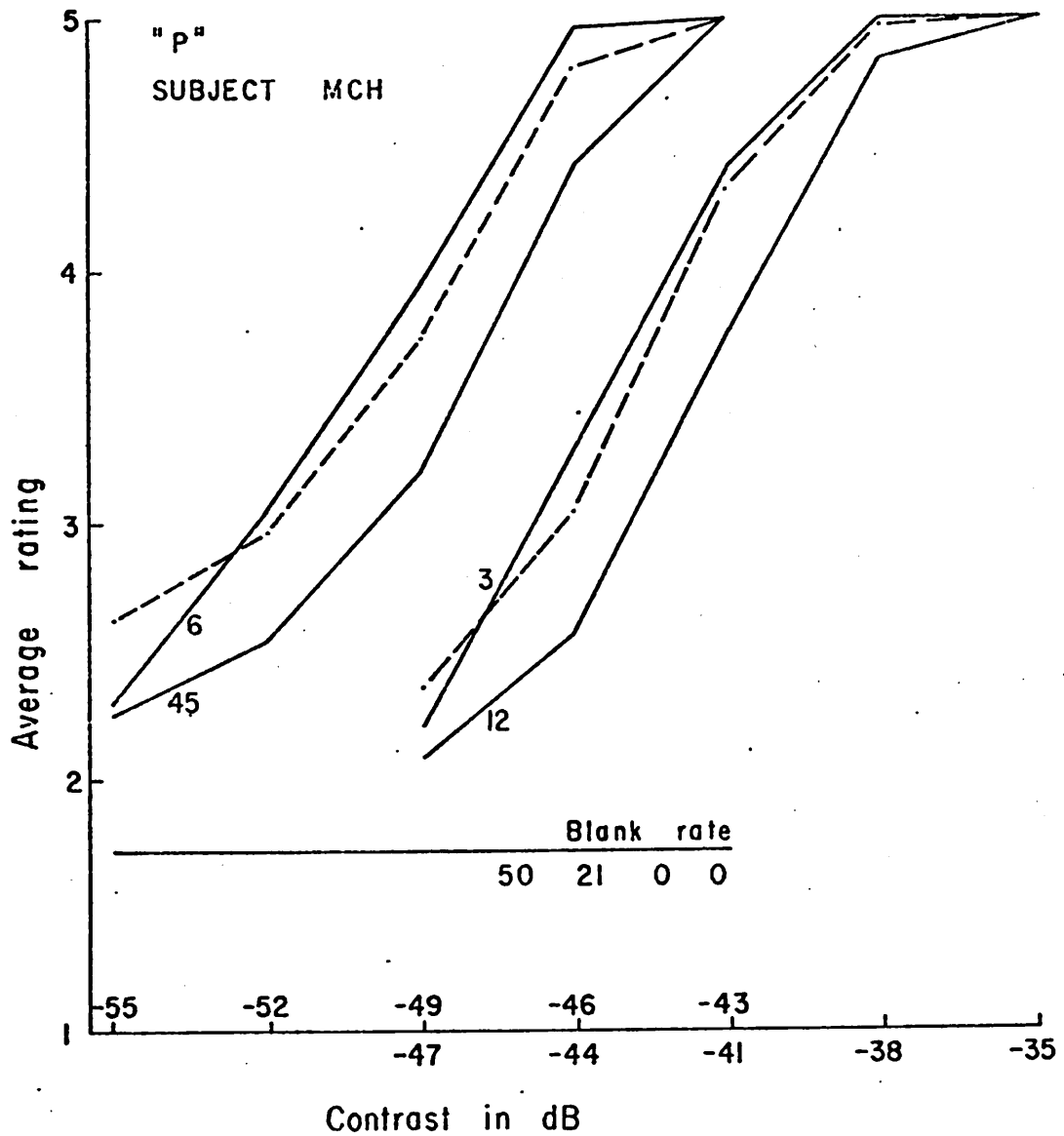


Fig. A.10. Data - "p" experiment. Groups of curves have been displaced laterally for clarity. Thus, two contrast scales are used, one for each group of curves.

The first type of patch, labelled p_1 , was identical to the f_1 (12.8 \sim /0) patch of the main experiment of this paper. Thus, patch "p₁ left" is that found in the upper left-hand corner of Fig. 4.1. Patch "p₁ right" is shown in the upper right-hand corner of Fig. 4.1. The second type of patch, p_2 , was obtained by deleting one-half cycle of a p_1 patch (the peak nearest the center of the visual field) and inverting the remainder. Thus, the left-side p_2 patch was essentially p_1 left moved leftward by one half cycle. The right-side p_2 patch was similar to p_1 right moved rightward by one half cycle.

Given these four patches (p_1 left, p_1 right, p_2 left, p_2 right), stimuli were constructed in a manner very similar to that of chapter 4. They were organized in groups of 5. Each group had a primary component which was one of the four patches. Each group also had a secondary component which was one of the two other-side patches or a blank. The contrast of a primary patch varied from stimulus to stimulus within a group. The contrast of a (non-blank) secondary patch remained constant within each group and always equalled the second-lowest contrast used for that patch when it was primary. Each group contributed to one of the psychometric functions of Fig. A.11.

In this experiment as in section 4.1 describing stimulus labels is equivalent to describing the stimulus set directly. We do so in the table below.

<u>LABEL DIGIT</u>	<u>MEANING AND POSSIBLE VALUES</u>
1	Nature of primary patch; 1 or 2. 1 meant type p_1 , 2 meant p_2 .
2	Summation code; 0 through 2. 0 meant the secondary component was a blank.

- 1 meant the secondary component was a p_1 patch on the other side of center from the primary patch.
- 2 meant the secondary component was a p_2 patch on the other side of center.
- 3 Contrast of primary patch; 1 through 5. 1 meant highest contrast, 5 lowest.
- 4 Position of primary patch; 1 or 2. 1 meant left-hand side, 2 right.

Each of the $2 \times 3 \times 5 \times 2 = 60$ different labels describes exactly one of the 60 non-blank stimuli presented in each experimental round.

Results: Only one set of useful data, Fig. A.11, was obtained in this experiment. Following the conventions described in section 4.2, psychometric functions are labelled with the two-digit number which formed the first two digits of the labels of all stimuli contributing to the curve. Each stimulus was viewed 52 times. Thus, since responses to mirror-image stimuli were averaged together, each data point in the figure represents 104 responses. The figure contains two groups of curves. The right-hand (left-hand) group is for those stimuli in which a p_1 (p_2) patch was primary. The circled points on the 10 and 20 curves show the subject's sensitivity to the p_1 and p_2 patches at their secondary role contrasts. Note that these sensitivities are virtually equal.

In this experiment as in chapter 4 it was possible to calculate precisely the behavior which should have resulted if the two components of a complex stimulus were processed independently by the visual system. Because the two circled points of Fig. A.11 are at the same height, only two such probability summation calculations were necessary, one for each type of primary patch. These calculations appear as dashed curves in the figure.

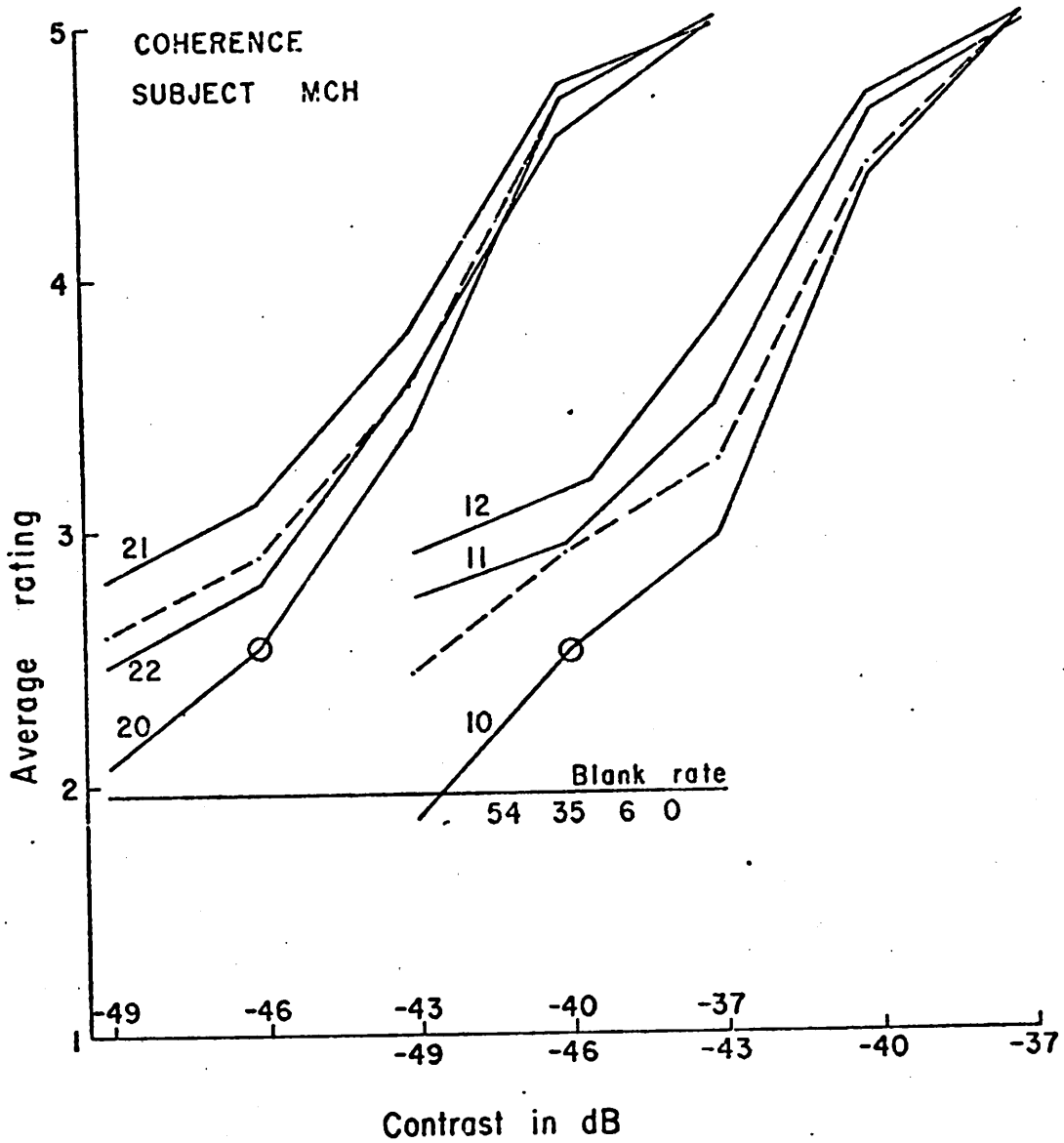


Fig. A.11. Data - "Coherence" experiment. Groups of curves have been displaced laterally for clarity.

Conclusions: When both primary and secondary components were of the same type, curves 11 and 22, the patches were in phase. When they were of different types, curves 12 and 21, the patches were 180° out of phase. When patch p_1 (p_2) was primary, in-phase (out-of-phase) patch to patch spacing was closer than out-of-phase (in-phase) spacing.

The subject showed a slight but consistent preference for out-of-phase spatial summation, regardless of whether or not this phasing meant closer spacing. This agrees with the results of Channel Shift-Phase I (section A.3). Thus, it appears that there may be a real preference for out-of-phase summation. However, the differences measured here are small and the result of Channel Shift-Phase I did not reoccur in Phase II. Thus, this result was considered inconclusive.

Note that curves 10, 11 and the neighboring dashed curve of Fig. A.11 represent the same stimulus conditions as do curves 10, 13 and neighboring dot-dashed curve of Figs. 4.2 through 4.6. However, in the present case the supra-probabilistic result is not as pronounced as it was in chapter 4. This finding is considered insignificant for two reasons. Curves 11, 22 and especially 12 do show supra-probabilistic summation indicating single channel breadth as discussed in chapter 5. Also, this experiment was not intended to verify the results of chapter 4 and, thus, spatial extent symmetry was not observed in the stimulus set. That is, full-field (two patch) stimuli appeared twice as often as did half-field stimuli. Nonetheless, the reader may wish to consider the present result in view of the findings of the next two experiments which also fail to repeat the strong supra-probabilistic finding of chapter 4.

A.7. Spacing (10/75)

The two 12.8 \sim /0 patches (left-side and right-side) at the top of Fig. 4.1 were used to construct the stimuli of this experiment. Each patch was presented by itself at various contrasts. Each patch was also displayed at the same set of contrasts but with the other patch added at contrast -45 dB.

Results: The data are plotted in Figs. A.12 and A.13. With one exception each stimulus was presented 64 times. Thus, because responses to mirror-image stimuli were averaged together, each data point represents 128 responses. The curve labelled "1" is for single patch stimuli. Curve "2" is for double patch stimuli. The circled point on curve 1 gives the subject's response to the patch at the contrast used in all of the two-patch stimuli. As usual, this response was used to make the probability summation calculation represented by the dashed line. For this reason this stimulus was presented more often than the others and its data point represents 384 responses.

Conclusions: Compare the present curves with curves 10, 13 and the dot-dashed curve of Figs. 4.2 through 4.6. The only difference in the stimuli is the set of contrasts used. However, the supra-probabilistic result of chapter 4 is, at best, weak here. It was concluded that, if both sets of data were to be believed, the presence of low frequency patches in the stimulus set of chapter 4 might have had an effect upon subject behavior.

A.8. Anticipation (11/75)

Three types of patches were used in this experiment. Each type could

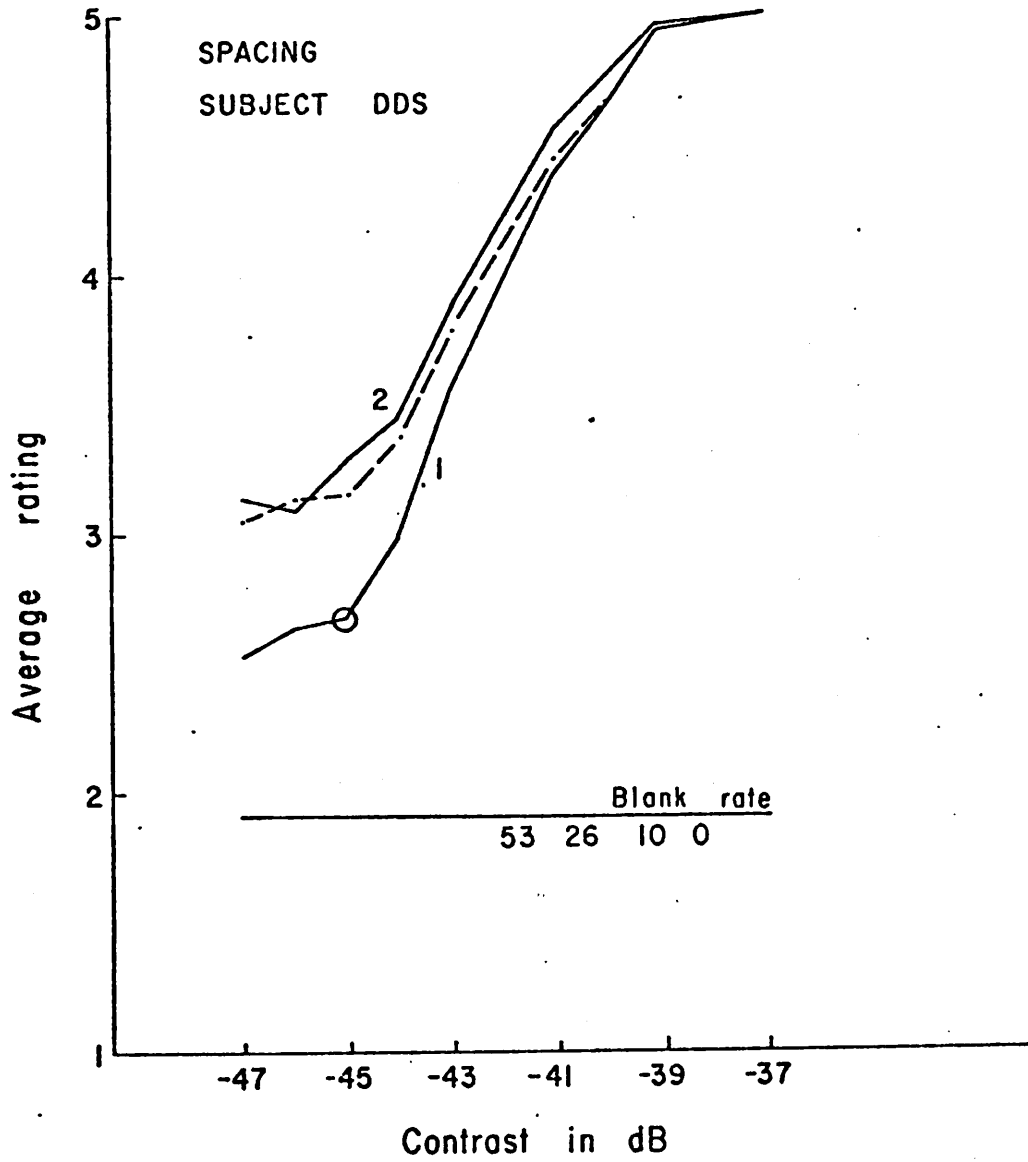


Fig. A.12. Data - "Spacing" experiment.

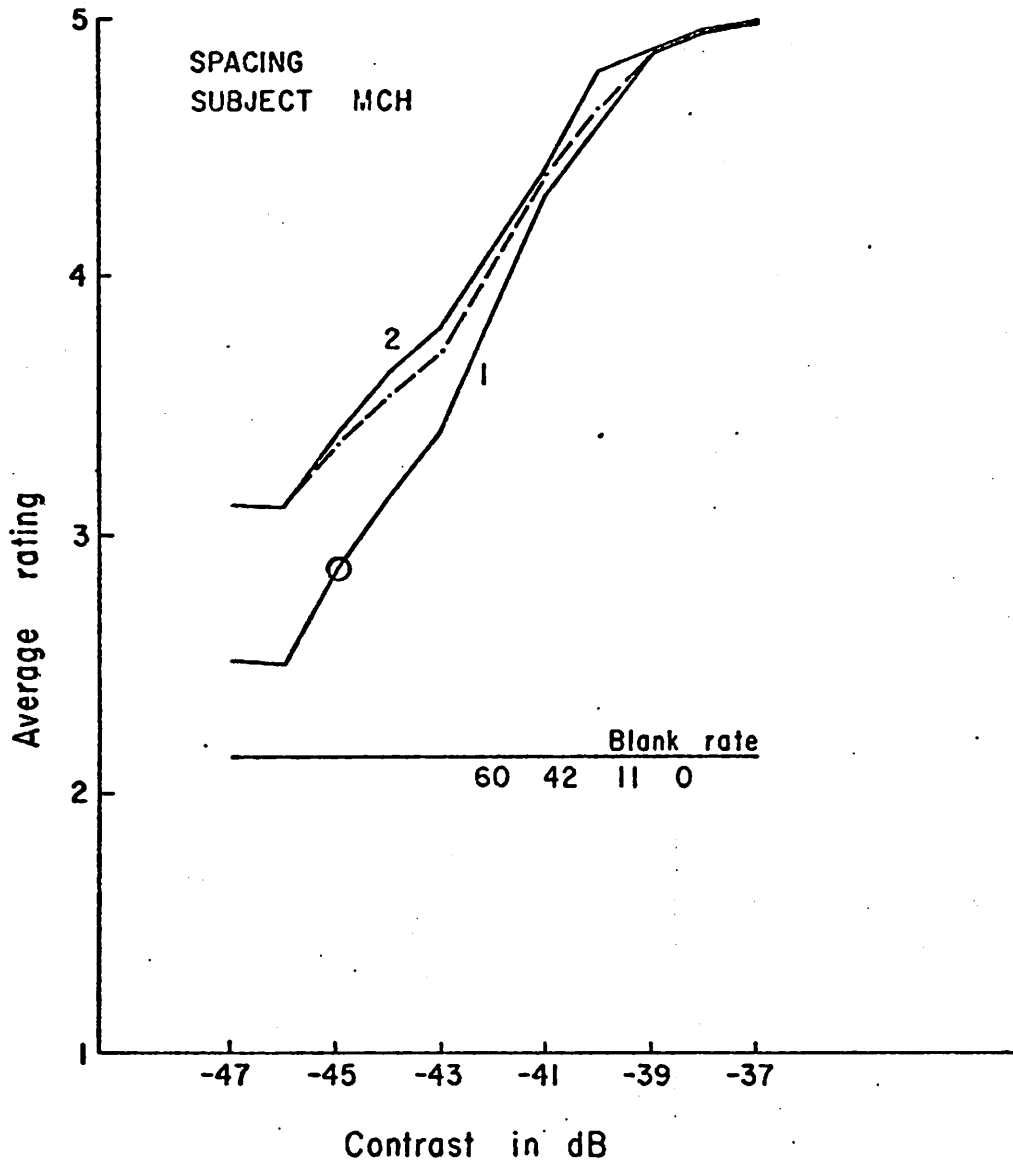


Fig. A.13. Data - "Spacing" experiment.

appear on either side of the visual field. Type p_1 patches were identical to the 12.8 \sim /0 patches of Fig. 4.1. Type p_2 patches were identical to the 4.3 \sim /0 patches of Fig. 4.1. Each p_3 patch was comprised of 2 cycles of a frequency $12.8/6 \approx 2.1$ \sim /0 sinusoidal grating. When both p_3 patches appeared together at the same contrast, the luminance distribution was that of 4.5 cycles at this frequency grating with the central peak removed.

One-patch and two-patch stimuli were constructed from the basic 6 patches in the manner of chapter 4 and section A.6. As was true in those experiments, the present stimulus set may be described in terms of the stimulus labels.

<u>LABEL DIGIT</u>	<u>MEANING AND POSSIBLE VALUES</u>
1	Nature of primary patch; 1, 2 or 3. 1 meant p_1 , 2 meant p_2 , 3 meant p_3 .
2	Summation code; 0 or 1. 0 meant the secondary component was a blank. 1 meant the secondary component was a patch of the same type as the primary component but on the other side of the visual field.
3	Position of primary patch; 1 or 2. 1 meant left-hand side, 2 right.

Unlike previous experiments, certain members of this stimulus set were presented more often than others. Stimuli whose labels had either 1 or 2 in the first digit (the two higher frequencies) were presented twice during each experimental round (8 times per day). Stimuli at the lowest frequency were presented once per round. This resulted in $2 \times (2 \times 2 \times 5 \times 2) + (1 \times 2 \times 5 \times 2) = 100$ non-blank stimuli per round.

Results: The data are plotted in Figs. A.14 and A.15. As usual, solid curves represent data and dashed curves represent probability summation calculations. The circled data points have the normal meaning and curve labels were derived from stimulus labels in the usual fashion. Each low frequency stimulus was presented 28 times and, thus, each data point on curves 30 and 31 represents 56 responses. Data points on curves 10, 11, 20 and 21 each represent 112 responses.

Conclusions: The right-hand group of curves in each figure is again comparable to curves 10, 13 and the neighboring dot-dashed curve of Figs. 4.2 through 4.6. As was true in sections A.6 and A.7, the supra-probabilistic result of chapter 4 is not clearly duplicated here. We concluded that the result of chapter 4 cannot be attributed to the presence of low frequency stimuli in the stimulus set.

Note that at the time of this experiment only two sets of data existed for the experiment of chapter 4 (Figs. 4.3 and 4.5, 6/75). We concluded that that experiment should be performed again, with 3 subjects, in order to determine whether the results of 6/75 were repeatable. As the reader has already seen, the data of 2/76 (Figs. 4.2, 4.4 and 4.6) confirmed the results of 6/75.

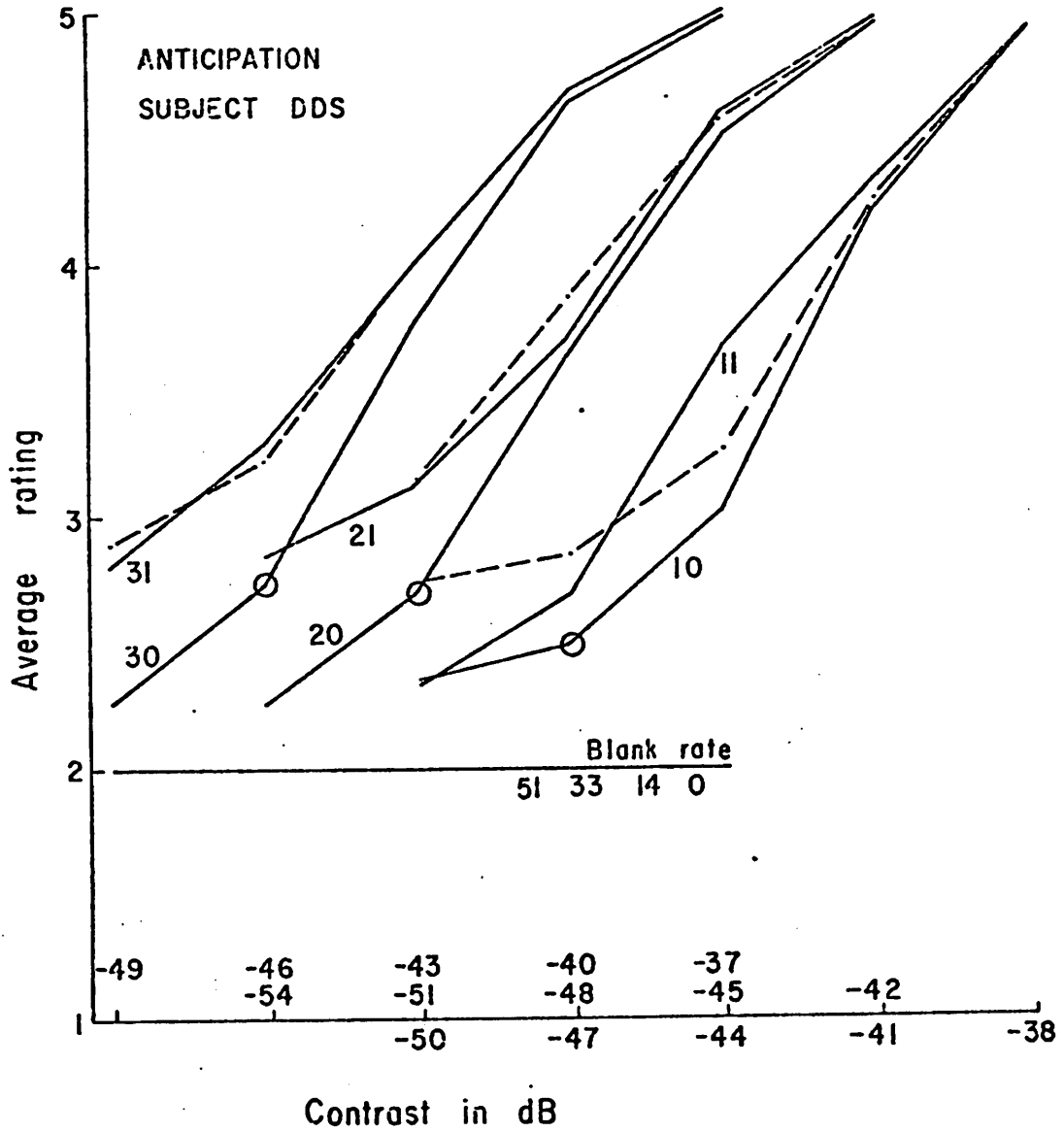


Fig. A.14. Data - "Anticipation" experiment. Groups of curves have been displaced laterally for clarity.

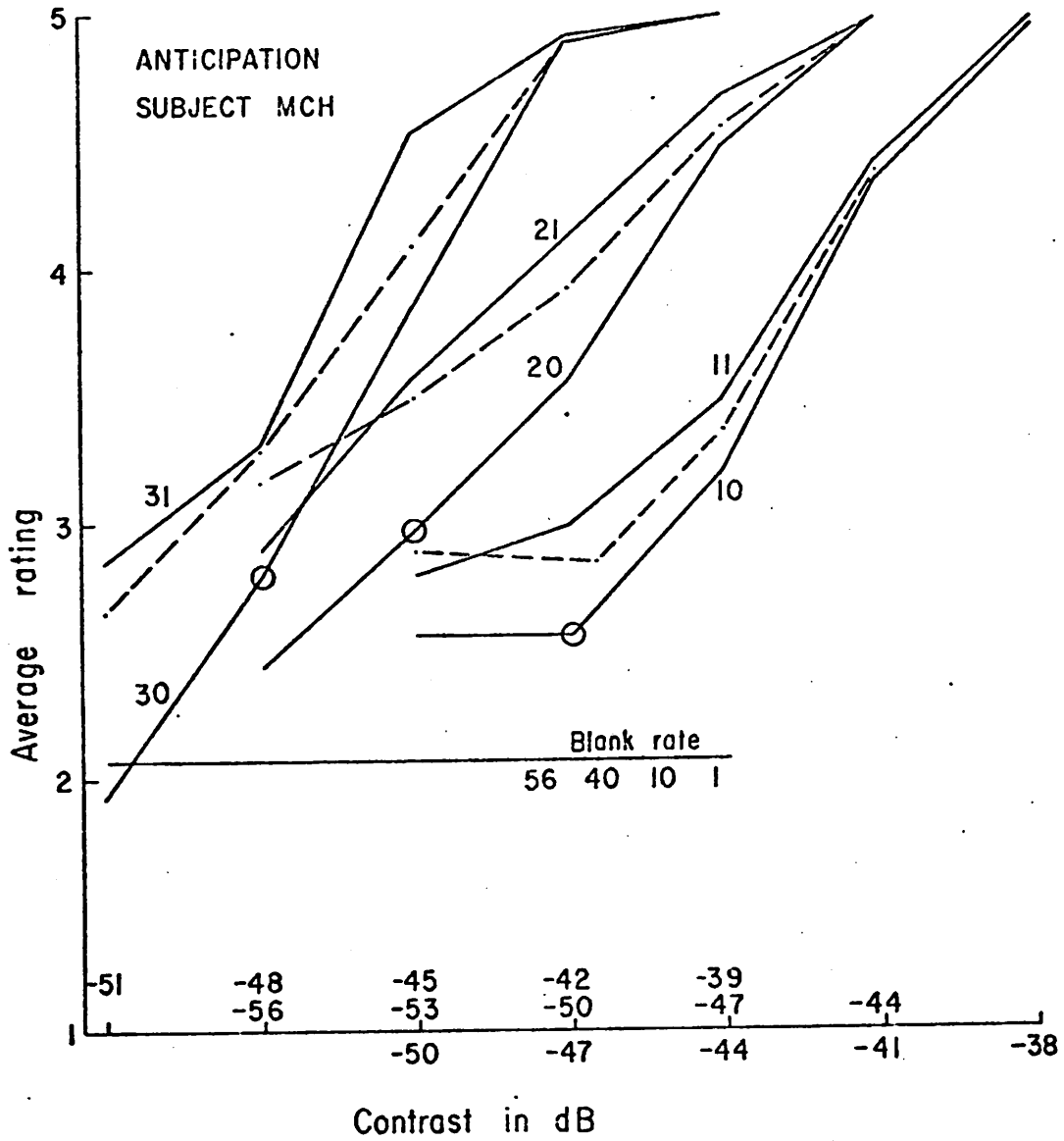


Fig. A.15. Data - "Anticipation" experiment. Groups of curves have been displaced laterally for clarity.

REFERENCES

- [1]. Ratliff, F., Mach Bands, San Francisco: Holden-Day, 1965.
- [2]. Fiorentini, A., "Mach Band Phenomena," Handbook of Sensory Physiology, Vol. VII/4: Visual Psychophysics, Jameson, D. and Hurvich, L. M., Ed., Springer-Verlag, 1972, Chapter 8, pp. 188-201.
- [3]. Sakrison, D. J., Communication Theory, New York: Wiley, 1968.
- [4]. Campbell, F. W. and Robson, J. G., "Application of Fourier Analysis to the Modulation Response of the Eye," J. Opt. Soc. Am., 54, 581, 1964.
- [5]. Campbell, F. W. and Robson, J. G., "Application of Fourier Analysis to the Visibility of Gratings," J. Physiol., London, 197, 551-566, 1968.
- [6]. Sachs, M. B., Nachmias, J. and Robson, J. G., "Spatial-Frequency Channels in Human Vision," J. Opt. Soc. Am., 61, 1176-1186, 1971.
- [7]. Kulikowski, J. J., Abadi, R. and King-Smith, P. E., "Orientational Selectivity of Grating and Line Detectors in Human Vision," Vision Res., Vol. 13, 1470-1486, Pergamon Press, 1973.
- [8]. Kulikowski, J. J. and King-Smith, P. E., "Spatial Arrangement of Line, Edge and Grating Detectors Revealed by Subthreshold Summation," Vision Res., Vol. 13, 1455-1478, Pergamon Press, 1973.
- [9]. Mostafavi, H. and Sakrison, D., "Structure and Properties of a Single Channel in the Human Visual System," Vision Res., Vol. 16, 957-968, Pergamon Press, 1973.
- [10]. Robson, J. G., Private Communication, 1972.
- [11]. King-Smith, P. E. and Kulikowski, J. J., "The Detection of Gratings by Independent Activation of Line Detectors," J. Physiol., London, 247, 237-271, 1975.

- [12]. Swets, J. A., Signal Detection and Recognition by Human Observers: Contemporary Readings, Swets, J. A., Ed., Wiley, 1964, Chapter 1, pp. 3-57.
- [13]. Robson, J. G., "Regional Variation of Contrast Sensitivity in the Visual Field," paper presented at the Spring Meeting of the Association for Research in Vision and Ophthalmology, 1975.